Optimal Planning of Parking Infrastructure and Fleet Size for Shared Autonomous Vehicles

Seongjin Choi[a], Jinwoo Lee[b,*]

[a]Department of Civil, Environmental, and Geo- Engineering, University of Minnesota, 500 Pillsbury Dr. SE, Minneapolis, MN 55455, USA
[b]Cho Chun Shik Graduate School of Mobility, Korea Advanced Institute of Science and Technology, 193, Munji-ro, Yuseong-gu, Daejeon 34051, Republic of Korea

ARTICLE INFO

Keywords:
Parking
Fleet Size
Shared Autonomous Vehicles
Optimization
Planning
Relocation

ABSTRACT

Parking is a crucial element of the driving experience in urban transportation systems. Especially in the coming era of Shared Autonomous Vehicles (SAVs), parking operations in urban transportation networks may inevitably change. Parking stations are likely to serve as storage places for unused vehicles and depots that control the level-of-service of SAVs. This study presents an Analytical Parking Planning Model (APPM) for the SAV environment to provide broader insights into parking planning decisions. Two specific planning scenarios are considered for the APPM: (i) Single-zone APPM (S-APPM), which considers the target area as a single homogeneous zone, and (ii) Two-zone APPM (T-APPM), which considers the target area as two different zones, such as city center and suburban area. S-APPM offers a closed-form solution to find the optimal density of parking stations and parking spaces and the optimal number of SAV fleets, which is beneficial for understanding the explicit relationship between planning decisions and the given environments, including demand density and cost factors. In addition, to incorporate different macroscopic characteristics across two zones, T-APPM accounts for inter- and intra-zonal passenger trips and the relocation of vehicles. We conduct a case study to demonstrate the proposed method with the actual data collected in Seoul Metropolitan Area, South Korea. We find that the optimal densities of parking stations and spaces in the target area are much lower than the current situation. Sensitivity analyses with respect to cost factors are performed to provide decision-makers with further insights.

1. Introduction

Parking is one of the crucial elements of the driving experience in urban transportation systems. However, as the number of vehicles in large cities around the globe increases rapidly, the lack of parking spaces has become a severe problem. From the perspective of the transportation system operator, the need to store vehicles is progressively increasing, which has led to the transformation of valuable real estate into parking garages (Nourinejad et al., 2018). Moreover, from the perspective of individual users, it is required to spend more time on the road searching for empty parking spaces, which eventually worsens overall traffic conditions (Lam et al., 2006). As a result, to improve the overall efficiency of the transportation system, it is necessary to study efficient parking operations.

A typical vehicle spends around 95% of its lifetime sitting in a parking space (Bates and Leibling, 2012). If we can utilize these unused vehicles to serve other travel demands, there is a possibility of reducing overall system costs, including vehicle ownership and parking operation. The idea behind 'Shared Autonomous Vehicles' corresponds to this possibility (Shaheen and Chan, 2016). Shared Autonomous Vehicles (SAVs) are the combination of growing shared mobility services (i.e., car-sharing and ride-hailing) and emerging autonomous vehicle technology Wang et al. (2022). SAVs can enable cost savings, provide convenience to users, and lead to sustainable transportation by reducing vehicle usage (Narayanan et al., 2020b; Ko et al., 2021; Jorge and Correia, 2013).

In the coming era of SAVs, it is inevitable to change parking operations in urban transportation networks (Zhang and Guhathakurta, 2017; Golbabaei et al., 2021). Parking stations are likely to serve as storage places for unused vehicles and depots that control the level-of-service of SAVs. As the market penetration of SAVs increases, there may be two main changes related to parking operations. First, parking demand is likely to be reduced because overall vehicle usage is likely to decrease (Zhang and Guhathakurta, 2017; Narayanan et al., 2020b). According to previous

*Corresponding author
Email addresses: chois@umn.edu (S. Choi); jinwoo@kaist.ac.kr (J. Lee)
ORCID(s): 0000-0001-7140-537X (S. Choi); 0000-0002-6692-9715 (J. Lee)

research, more than 25% of individuals are willing to give up their vehicle ownership given the availability of an SAV alternative (Menon et al., 2019). Also, one SAV can replace from 1.93 to potentially ten conventional individually owned vehicles (Lokhandwala and Cai, 2018; Fagnant and Kockelman, 2014). Second, the spatial distribution of parking stations (parking lots) may be fundamentally rearranged (Zhang, 2017). It may be possible to relocate parking stations outside the city center; SAVs may travel from parking stations to passengers because SAVs can travel at a low cost (Kröger and Kickhöfer, 2017).

Despite many studies on parking operations with the dominance of SAVs, most studies have used simulation-based approaches. However, such approaches have limitations. They require massive effort and cost (i) to acquire appropriate and detailed data and (ii) to set up and run computationally heavy simulations to obtain appropriate solutions. Consequently, solutions from simulation-based approaches rely highly on the quality of collected data so that proper solutions can only be found when a sufficient amount of explanatory data exists for simulation. Moreover, simulation results for a particular situation are difficult to generalize and apply to different situations. The findings from the simulation results from a certain city cannot be directly applied to another city's planning problem, since the results are 'site-specific.'

In this study, to overcome the limitations of simulation-based approaches, we present an Analytical Parking Planning Model (APPM) with SAVs. Usually, analytical models focus primarily on functional systemic relationships between planning variables and the objective function. Based on the mathematical approximations presented in Daganzo and Ouyang (2019b), we can simplify the parking operation of urban transportation systems with SAVs. By using this, only macroscopic data of target cities (or area) is needed, instead of detailed data required in simulation analysis. Analytical models are used to identify generally applicable insight on planning decisions; if detailed data are available, this insight can be further improved and refined through simulations for target areas if necessary. Similarly, the proposed model in this study explicitly explains the inter-relationship among the parking planning variables together with the other important exogenous factors, such as land cost and vehicle operating costs, in a closed form. The required data to use the proposed model is much simpler than the data required for simulation-based approaches, which overcomes the first limitation of simulation-based approaches. Also, using a closed form can overcome the significant computation inefficiency of simulation-based approaches, since the solutions can be calculated by one shot.

We use two scenarios to describe parking operations in a given urban traffic network, the *Single-zone Analytical Parking Planning Model* (S-APPM) and *Two-zone Analytical Parking Planning Model* (T-APPM) to properly design a model structure that describes the parking operation with SAVs. S-APPM considers the target region a single zone with macroscopic characteristics for parking planning decisions. As a result, the derived optimal parking planning decisions are assumed to be the same in all sub-regions in the target region. On the other hand, T-APPM considers the target region as two distinguishable zones, usually represented as a city center and suburb. As a result, it is possible to consider the effects of different macroscopic characteristics of each zone (such as passenger demand, land cost, average speed, etc.) on parking planning decisions. Also, we conduct case studies for each model to demonstrate the sensitivity of the model on the cost factors and the effect of relocation between zones on parking planning. The contributions in this paper are summarized as follows:

- To the best of our knowledge, it is the first to propose analytical models for parking planning, especially with SAVs.
- We formulate the parking operation problems with total operating cost as an objective function, and we carefully derive the parking operation variables in the objective functions for S-APPM (Section 3) and T-APPM (Section 5). The models explicitly explain the inter-relationship among the variables together with the other important exogenous factors.
- We conduct the case studies to give general insights on the proposed model with extensive sensitivity analyses on cost parameters for each parking operation variable. (Section 4, Section 6)

The organization of this paper is as follows. We present S-APPM in Section 3 and solve the objective function to derive the decision variables and parking operational variables. Then, in Section 4, a case study of Seoul, South Korea, is presented to further elaborate on our findings for S-APPM. T-APPM is presented in Section 5 by extending S-APPM with the relocation of vehicles between two zones. A case study of the Seoul Metropolitan Area, including Seoul and other cities near Seoul, is presented in Section 6. Finally, in Section 7, we conclude our study by summarizing the key findings and contribution of this study, as well as addressing limitations and proposing future research. The notations used in this paper are listed in Appendix A.

2. Literature Review

The emergence of shared autonomous vehicles (SAVs) is expected to bring significant changes to urban transportation systems, including the way in which parking infrastructure is planned and managed. As SAVs are expected to operate more efficiently and have higher utilization rates than conventional vehicles, the demand for parking spaces may decrease in some areas while increasing in others. This presents a unique challenge for urban planners and policymakers, who must optimize parking infrastructure to meet the changing demands of SAVs. However, despite the increasing interest in SAVs, the literature on parking optimization in the context of SAVs is still relatively limited.

Several studies have examined the potential impact of SAVs on urban transportation. Fakhrmoosavi et al. (2022) conducted a study to explore the effects of various parking strategies on Shared Autonomous Vehicle (SAV) fleets, taking into account the escalating demand for ride-hailing services. The study highlighted the potential of employing parking pricing as a tactical instrument to incentivize passengers to choose shared rides. This, in turn, could alleviate traffic congestion that arises from vehicles searching for parking spaces. Yan et al. (2020) presented a microsimulation study on the performance of SAV fleets in the Minneapolis-Saint Paul region, examining the impacts of trip densities and parking restrictions. Results suggest that SAVs can serve at most 30 person-trips per day with less than 5-minute wait time, generating 13% more vehicle-miles traveled (VMT), but with dynamic ride-sharing (DRS), SAV VMT fell by 17%. The paper also estimates the potential energy savings and emissions reductions with hybrid and battery-electric SAV fleets. Oh et al. (2020) examined the potential impacts of Automated Mobility-on-Demand (AMOD) in Singapore through agent-based simulation. The study utilizes an activity-based model system to model demand and a traffic simulator to model the operations of the AMOD fleet, analyzing the impacts of AMOD from the perspectives of transportation planner, fleet operator, and user. The findings suggest that an unregulated introduction of AMOD could increase network congestion and Vehicle-Kilometers Traveled (VKT), highlighting important policy implications for future deployments of AMOD.

Other studies have focused specifically on the impact of SAVs on parking demand and infrastructure. Zhang et al. (2015) used an agent-based simulation model in a hypothetical city to estimate the potential impact of an SAV system on urban parking demand. They found that the use of SAVs could significantly reduce parking demand, particularly in areas with high population density. Similarly, Zhang and Guhathakurta (2017) explored the potential impact of SAVs on urban parking demand using an agent-based simulation model. The study estimates that SAVs could eliminate up to 90% of parking demand for clients with a low market penetration rate of 2%. The results also suggest that different SAV operation strategies and client preferences may result in different spatial distribution of urban parking demand. Azevedo et al. (2016) used SimMobility to analyze the impact of demand and supply of autonomous mobility on demand (AMoD) in Singapore. This study used an optimization algorithm to solve the facility location problem to find optimal locations for a fixed number of parking stations. The results showed that the use of SAVs could significantly reduce the number of parking stations required, while still providing adequate service levels to users. Kondor et al. (2018) considered the distance an SAV can travel to the nearest parking station as a constraint in estimating the required number of parking stations. They found that the use of SAVs could reduce the number of parking stations required, particularly in areas with high population density. Okeke (2020) presented a case study at the University of West England to analyze the impacts of autonomous vehicle technology on parking operations. They used agent-based simulation and a parking model to study the relocation of parking stations outside city centers. They found that SAVs would allow parking stations to be relocated outside city centers, reducing congestion and improving accessibility. Zhang and Wang (2020) analyzed the potential impact of SAVs on parking demand reduction in Atlanta by developing an agent-based simulation model. The study examines the spatial and temporal parking reduction trends with mixed travel modes from 2020 to 2040 and suggests that parking demand could decrease by over 20% after 2030, particularly in core urban areas. However, parking demand in residential zones may double, creating transportation equity concerns, and parking relocation may result in a considerable amount of empty Vehicle Miles Traveled (VMT). The paper suggests that proactive policymakers will need to modify land use regulations and travel demand management policies to reap the benefits brought by SAVs and mitigate associated issues. Wang and Zhang (2021) examined the impact of urban form on the performance of SAVs through simulation experiments using data collected from 286 cities. The study identifies critical urban form measurements correlated with SAV performance and suggests that SAVs are more efficient and generate less Vehicle Miles Traveled (VMT) in denser cities with more connected networks and diversified land use development patterns. The results provide insights for land use and transportation policies to mitigate the adverse effects of SAVs and generalize existing SAV simulation results to other U.S. cities.

However, the majority of previous studies have focused on the impact of SAVs on urban transportation systems and parking infrastructure, using agent-based large-scale simulations that require significant computational resources. While these studies have provided valuable insights into the potential benefits and challenges of SAVs, they may not be practical for decision-makers who require more efficient and effective methods to optimize parking infrastructure.

In light of the challenges associated with using large-scale simulations for SAV parking optimization, there is a need for more efficient and effective methods. Analytical modeling approaches offer an attractive alternative, as they can provide general insights into parking optimization while requiring fewer and less detailed inputs.

Daganzo and Ouyang (2019a) proposed a framework to model transit systems, including shared and non-shared systems. The framework provides approximate formulas for many cases of interest but is not space-tracking and is deterministic. The framework can be used to analyze the performance and efficiency of various transit systems. Several recent studies have used analytical modeling for shared mobility, following Daganzo and Ouyang (2019a). For example, Bahrami et al. (2022) analyzed the benefits of offering solo and pool services for on-demand ride-hailing, while Kim and Roche (2021) proposed an optimization model for flexible-route bus services in low to mid-demand density areas. Daganzo et al. (2020) examined the benefits of introducing upper bound guarantees to detour distances in ride-sharing services, while Kim et al. (2019) explored the benefits of flexible-route bus systems serving passengers at their doorsteps in areas with low demand densities. Finally, Papanikolaou and Basbas (2021) examined Demand Responsive Transport (DRT) services as a viable mobility service for low demand interurban areas. These studies provide insights into the role and potential markets of shared mobility services and the need for viable business models.

Analytical modeling offers a more efficient and effective approach to parking optimization in the context of SAVs, as it allows for the development of general and insightful designs that require fewer and less detailed inputs than large-scale simulations. Such models can provide decision-makers with the tools and knowledge they need to optimize parking infrastructure in a more practical manner. However, the literature currently lacks an overarching model that can encompass a large family of systems, making it difficult to compare and evaluate different approaches in a generalized and comprehensive way. The proposed Analytical Parking Planning Model (APPM) presented in this study aims to fill this gap by providing a general analytic framework that can be used to model the steady-state performance of various demand-responsive transit systems, including SAVs. This framework can help mobility service providers answer important questions related to service offerings, service quality, resource acquisition, and cost management while meeting the level of service target.

3. Single-Zone Analytical Parking Planning Model

To be consistent with the previous demand-responsive shared mobility model without the parking state (Daganzo and Ouyang, 2019a), we consider a given homogeneous target region with a size of R [km^2] simplified into a single zone with uniform origin and destination (O-D) demands λ_t [$\text{veh}/\text{km}^2/\text{hr}$], which vary by time window t. Time windows associated with the daily maximum and minimum demands are designated by $t_{\lambda_{max}}$ and $t_{\lambda_{min}}$, respectively. Figure 1 shows the operation scenario for parking stations with SAVs. The blue circles represent the parking stations installed in the target region. The density of the parking stations is denoted as x [$\text{stations}/\text{km}^2$], parking spaces in the target region is denoted as y [$\text{spaces}/\text{km}^2$], and the average parking spaces per station z [$\text{spaces}/\text{station}$] is y/x. The red line represents a single passenger demand in the scenario. When a passenger demand is generated, an SAV in the nearest not-empty parking station is assigned to the passenger, cruises to the origin location of the passenger, and picks up the passenger. After pickup, the SAV delivers the passenger to the destination. Then, the SAV cruises to the nearest not-full parking station and awaits the next passenger assignment. We assume that the target region is homogeneous, which means that it has homogeneous conditions and variables, such as uniform O-D demand and uniformly distributed parking stations and spaces. We believe that this is a reasonable simplification given the homogeneous nature of the zone we are modeling and the relatively large study site used in our case study.

3.1. Optimization Framework

The objective of this model is to minimize total operating cost in the target region by determining three variables related to parking space and SAV fleet planning:

- x – density of parking stations [$\text{stations}/\text{km}^2$]
- y – density of parking spaces [$\text{spaces}/\text{km}^2$]
- m – number of SAV fleets [veh]

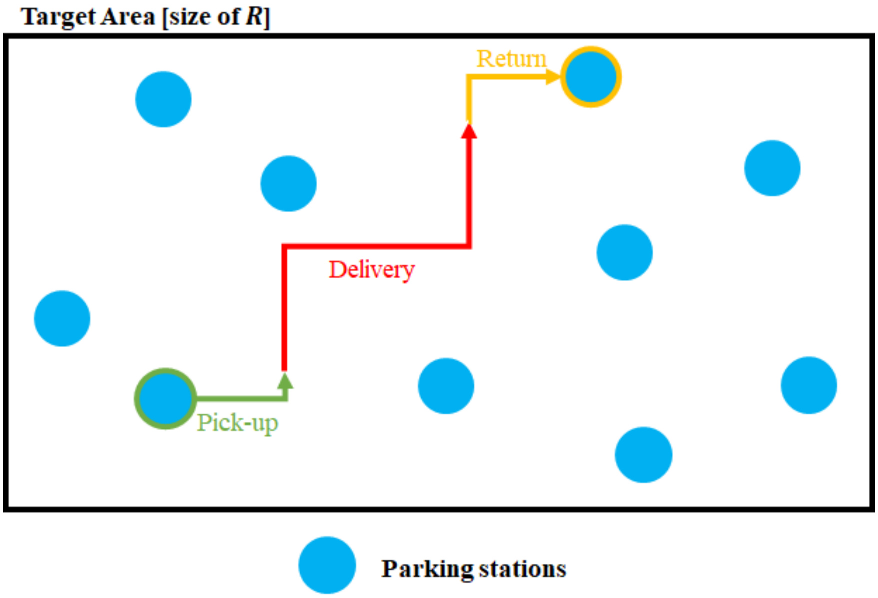

Figure 1: Operational scenario of parking stations with Shared Autonomous Vehicles. Blue circles represent parking stations. SAV moves from one parking station to the origin location of the passenger (green), picks up the passenger, and delivers the passenger to the destination (red); SAV then moves to the nearest parking station (yellow).

The objective function of the parking operation consists of three different operation costs: (i) parking station costs, (ii) parking space costs, and (iii) fleet costs. The objective function J of the parking operation [\$/day] is to minimize the overall daily average operation cost ($Cost$), formulated as a function of the planning variables, x, y, and m, as follows:

$$J = \min_{x,y,m} Cost(x, y, m) = \min_{x,y,m} \left(C_x x R + C_y y R + C_m m \right), \tag{3.1}$$

where C_x refers to the daily average operation cost of each parking station, such as the rental cost or prorated purchase cost for the land and built infrastructure on it, except for the variable costs depending on the number of parking spaces at the station [\$/stations/day]; C_y stands for the daily operation cost of a unit parking space, except for the cost components included in C_x [\$/spaces/day]; and C_m indicates the daily operation cost of each vehicle [\$/veh/day], including a wide range of operating costs from purchasing costs, maintenance costs, energy/fuel costs, and driver expenses, to other service-related costs such as online platform costs.

For passenger convenience, measures of Level-Of-Service (LOS) of SAV operation related to passenger waiting time can be used as constraints. In demand-responsive mobility services, ensuring short assigning time, i.e., the elapsed time between a call and vehicle assignment, and assigned time, i.e., the waiting time between the assignment and passenger pickup, is important (Lees-Miller, 2016; Daganzo and Ouyang, 2019a). In SAV operations, as an assignment can be automatically conducted in a top-down manner from the control center, assigning time can be ignored. Thus, we take into account a LOS constraint that restricts only the average assigned time so that it does not exceed a pre-selected threshold, as in:

$$T_{A,t} \leq T_0, \forall t. \tag{3.2}$$

where $T_{A,t}$ is the average passenger waiting time, only consisting of assigned time, in time window indexed by t (in state A), that means “Assigned”, and T_0 is the threshold, the maximum allowed average passenger waiting time. This constraint is likely to be binding when travel demand is the highest in $t_{\lambda_{max}}$.

Last, it is impossible to park additional SAV more than $z = x/y$ at one parking station. This constraint is especially important when travel demand is the lowest in $t_{\lambda_{min}}$.

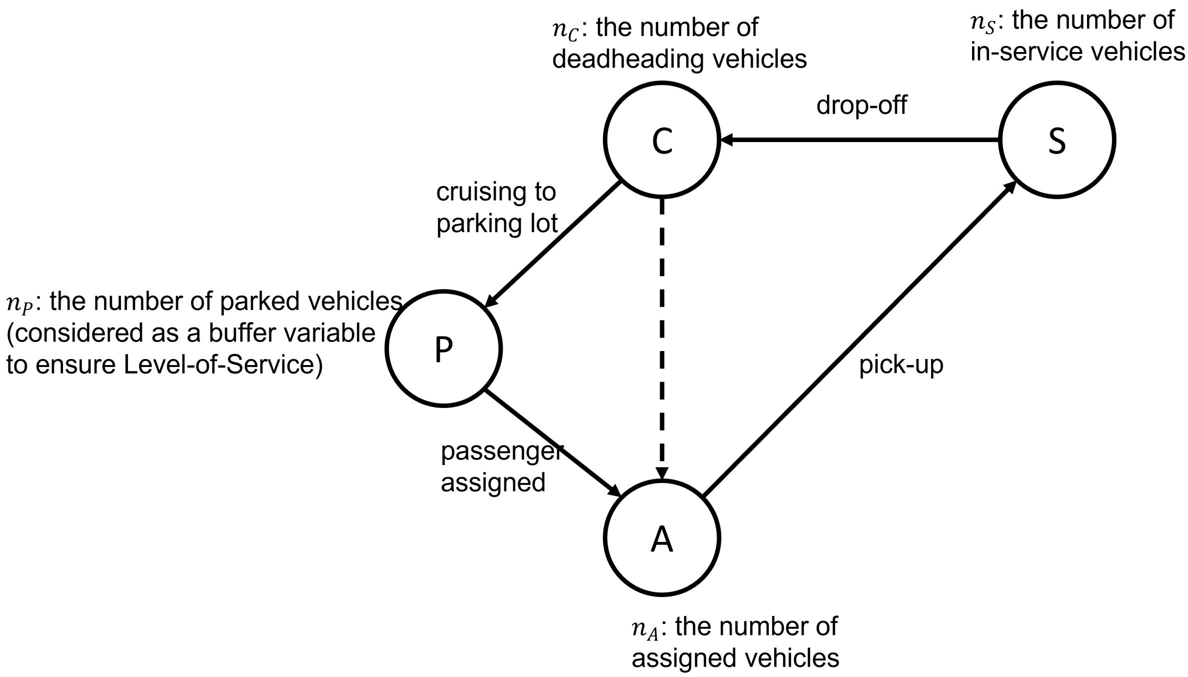

Figure 2: Workload transition network representation of Single-zone Parking Planning Model (S-APPM). Circles represent the states, and the directed lines represent transitions between states. The dotted line (from C to A) is also possible in reality.

3.2. SAV Operation Model with Parking

To analytically formulate the LOS constraint as a function of the decision variables, we model SAV operations with parking planning as a workload transition network graph presented in Figure 2, inspired by the demand-responsive transit model proposed by Daganzo and Ouyang (2019a). The nodes of the graph in Figure 2 represent the operational states of SAVs, and the links stand for the transitions between them. An SAV is in either of four different states:

- P (Parked): the vehicle is idle and parked at the parking station;
- A (Assigned): once assigned to a passenger, the vehicle is moving to the passenger's current location from the previous parking station;
- S (Serving): the vehicle is delivering a passenger from his/her origin to destination;
- C (Cruising to return): After serving, the empty vehicle is cruising to the nearest not-full parking station.

Once a passenger engages service, we assume that a vehicle parked at the nearest non-empty station is assigned to the passenger, resulting in a change of operational state of the assigned vehicle from state P to state A ($P \rightarrow A$). Then, the assigned vehicle moves from the parking station to the origin of the passenger's trip ($A \rightarrow S$). When the vehicle arrives at the origin of the passenger's trip, the vehicle picks up the passenger and travels from origin to destination. The operational state changes from *Serving* S to *Cruising to return* C when the passenger gets off the vehicle ($S \rightarrow C$). After completion of the passenger's trip, the vehicle moves to the nearest not-full parking station and waits for the next assignment ($C \rightarrow P$).

In reality, it is also possible to allocate a new passenger request to the nearest vehicle in state C. In other words, vehicles that are moving to a parking station can be allocated to another passenger's request before they arrive at the parking station, as represented by the dotted line in Figure 2. However, for the mathematical simplicity of this model, we neglect this state transition. Nonetheless, the proposed model can provide a lower bound on the efficiency of the system because including the state transition from state C to state A will increase the overall efficiency of the SAV system through extra operational flexibility. The lower bound can provide us with information about the minimum benefits of SAV operations with optimal parking and fleet planning, which is particularly important to determine the feasibility of introducing the system. Forcing SAVs to park between trips might add empty VMT (i.e., miles

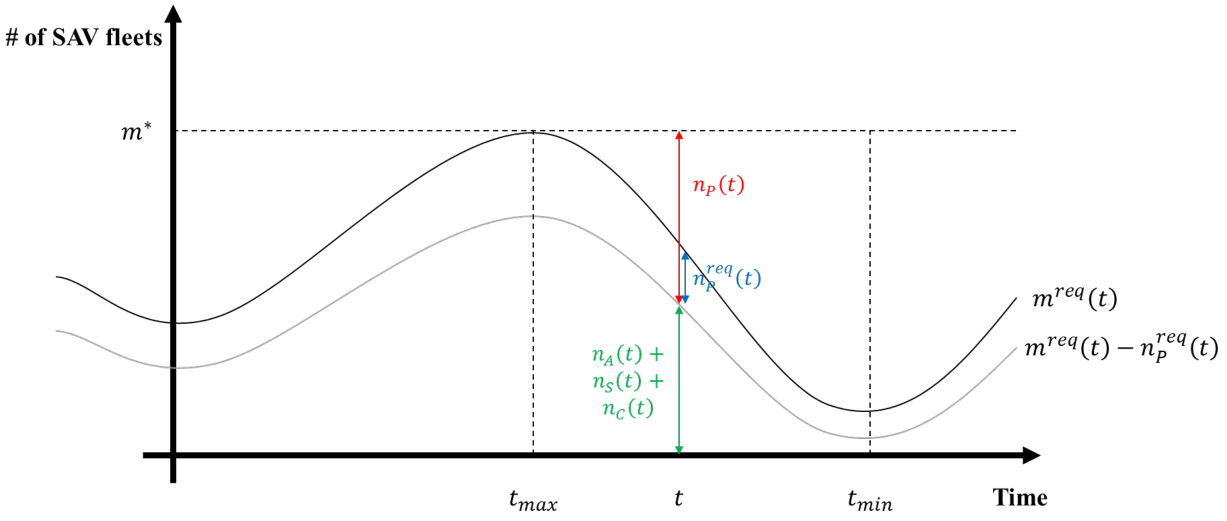

Figure 3: Graphical expression of change of the number of SAV fleets over time. $t_{\lambda_{max}}$ represents the time window associated with maximum demand and $t_{\lambda_{min}}$ represents the time window associated with minimum demand. At a given time window t, the red portion represents the number of SAV fleets parked at parking stations ($n_P(t)$), the blue portion represents the required number of SAV fleets in parking station, and the green portion represents the number of SAV fleets actively running on the roads.

traveled without a passenger) to the system and inflate congestion. This issue can be addressed by adopting approaches such as Dynamic Ride Sharing, as suggested by Yan et al. (2020), or by introducing state-specific cost variables to minimize eVMT. Dynamic Ride Sharing enables the real-time matching of passenger requests with available SAVs, thus reducing eVMT and improving the overall efficiency of the system. On the other hand, introducing state-specific cost variables allows for more targeted optimization, accounting for the costs associated with eVMT and parking, and helping to further minimize empty vehicle miles traveled. Both strategies have the potential to alleviate congestion and improve the efficiency of SAV deployments in urban environments. However, implementing these approaches may also increase the complexity of the model and require more sophisticated optimization techniques. Future research could explore the integration of these strategies to develop more accurate and practical solutions for SAV deployment in urban transportation systems.

The fleet size in each state in the given time window, denoted by $n_A(t)$, $n_S(t)$, $n_C(t)$, and $n_P(t)$, respectively, vary depending on the time-dependent passenger demand λ_t, as well as the decision variable.

$$m(t) = n_A(t) + n_S(t) + n_C(t) + n_P(t), \tag{3.3}$$

The required number of fleets in time window t, needed to ensure user LOS, can be defined as the summation of the required number of fleets in each state to ensure the LOS as shown in Equation 3.4:

$$m^{req}(t) = n_A^{req}(t) + n_S^{req}(t) + n_C^{req}(t) + n_P^{req}(t), \tag{3.4}$$

where $n_A^{req}(t)$, $n_S^{req}(t)$, $n_C^{req}(t)$, and $n_P^{req}(t)$ refer to the required number of fleets in state A, S, C, and P , respectively.

As shown in Figure 3, the SAV fleet size m is constant over the whole day, so the minimum required fleet size m^* is equal to the maximum required number of SAVs among all the time windows of the day, i.e., the required fleet size in time window $t_{\lambda_{max}}$ when the demand is at the maximum level, as shown in Equation 3.5:

$$m^* = \max_t (m^{req}(t)). \tag{3.5}$$

The three components on the right-hand side of Equation 3.4, $n_A^{req}(t)$, $n_S^{req}(t)$, and $n_C^{req}(t)$, can be expressed based on Little's Law with exogenous and endogenous planning variables. In other words, the fleet sizes in each state are calculated by multiplying the demand ($\lambda_t R$) by the expected time spent in each state (T_A, T_S , and T_C). The last component, $n_P^{req}(t)$, is a buffer to ensure that there are not too many (not to exceed the parking space limit at a station) and not too few (to ensure the level-of-service by guaranteeing an idle vehicle to assign to any demand generated nearby) vehicles at the parking station. $n_P^{req}(t)$ can be derived based on the variance of the vehicle inflow and outflow at each parking station.

First, the fleet size in state A in time window t, $n_A^{req}(t)$, is derived as follows:

$$n_A^{req}(t) = \lambda_t R T_{A,t}, \tag{3.6}$$

where, as used in Equation 3.2, SAVs' assigned time $T_{A,t}$ is equal to the average passenger waiting time.

In some cases, especially when passenger demand is high, it is possible that the parking station nearest to the origin of the passenger does not have an idle SAV to serve passenger demand. In this case, it is required to send an idle SAV from the second-nearest parking station, and so on. As a result, we consider a confidence level p, defined as the probability that a passenger is served by an SAV from the nearest parking station. The number of fleets in state A can be expressed as Equation 3.7. If p is sufficiently high, $p \to 1$, the probability that an SAV from the i-th nearest parking station is assigned to a passenger, $(1-p)^i \cdot p$, becomes almost zero, so we ignore the corresponding terms.

$$\begin{aligned} n_A^{req}(t) &= \lambda_t R \left(pT_{A,t}^1 + (1-p)\left(pT_{A,t}^2 + (1-p)(pT_{A,t}^3 + (1-p)(\cdots) \right) \right) \\ &\approx \lambda_t R \left(pT_{A,t}^1 + (1-p)\left(pT_{A,t}^2 \right) \right) \\ &= \lambda_t R \left(pT_{A,t}^1 + (1-p) \cdot \alpha p T_{A,t}^1 \right) \\ &= \lambda_t R T_{A,t}^1 \left(p + \alpha p - \alpha p^2 \right) \end{aligned} , \tag{3.7}$$

where $T_{A,t}^i$ refers to the average travel time from the i-th nearest parking station to the origin of the passenger, and α is the incremental ratio of the travel time, i.e., $\alpha \equiv T_{A,t}^2 / T_{A,t}^1$. From Equations 3.6 and 3.7, $T_{A,t}$ is $T_{A,t}^1(p + \alpha p - \alpha p^2)$. Note that this assumption only considers the two nearest parking places. Since we assume p is close to 1, this implies a high probability of finding a parking spot within the two nearest parking places. If p is small and the vehicle has to come from a faraway parking station, it would decrease the level-of-service. Therefore, we reasonably assume that we only consider the two nearest parking places for this study, but this assumption can be modified to better fit specific applications.

Second, the number of fleets in state S, $n_S^{req}(t)$, is derived as follows:

$$n_S^{req}(t) = \lambda_t R T_{S,t} = \lambda_t R \frac{l_t}{v_t}. \tag{3.8}$$

As $T_{S,t}$ is the average travel time from origin to the destination for all passengers in time window t, it can be simply derived with average trip length l_t [km] considering the circuity of roads and the average speed v_t [km/hr].

Third, the fleet size in state C in time window t is formulated as follows:

$$n_C^{req}(t) = \lambda_t R T_{C,t}, \tag{3.9}$$

where $T_{C,t}$ is the expected time a vehicle spends in state C. $T_{C,t}$ is the travel time from the destination of the passenger to the nearest parking station. When passenger demand is low, it is possible that the parking station nearest the destination of the passenger will be full and there are no parking spaces left. In this case, it is required to send the SAV fleet to the second-nearest parking station, and so on. As a result, we consider a confidence level q, the probability that the nearest parking station is not full. The fleet size in state C in time window t can be expressed as follows:

$$\begin{aligned} n_C^{req}(t) &= \lambda_t R \left(qT_C^1 + (1-q)\left(qT_C^2 + (1-q)(qT_C^3 + (1-q)(\cdots))\right)\right) \\ &\approx \lambda_t R \left(pT_C^1 + (1-q)\left(qT_C^2\right)\right) \\ &= \lambda_t R \left(qT_C^1 + (1-q)\cdot \alpha q T_C^1\right) \\ &= \lambda_t R T_C^1 \left(q + \alpha q - \alpha q^2\right) \end{aligned}, \tag{3.10}$$

where $T_{C,t}^i$ refers to the average travel time from the destination of the passenger to the i-th nearest parking station and α is the incremental ratio of travel time between $T_{C,t}^2$ and $T_{C,t}^1$, which is equivalent to $\alpha \equiv T_{A,t}^2/T_{A,t}^1$ in Equation 3.7. Based on the assumption of uniformly distributed O-D demands and parking station, $T_{C,t}^1$ is equal to $T_{A,t}^1$.

Finally, the required fleet size in state P, $n_P^{req}(t)$ can be derived by accounting for the variance of the number of idle vehicles parked at each parking station. Variances of vehicles coming into a parking station and vehicles going out of a parking station are $\lambda_t RHI/x$ each, where H is the length of the time window, and I is the mean-to-variance ratio of the number of vehicles parked at each parking station. To be more specific, $\lambda_t RH$ is the mean origin demand and destination demand for the whole area, $\lambda_t RH/x$ is the mean origin/destination demand for one parking station. We use the mean-to-variance ratio I to calculate the variance as $\lambda_t RH/x$ (I is assumed to be 1 in the case study by assuming the O-D event follows Poisson distribution). Consequently, the variance of vehicle number at a parking station during a time window is $2\lambda_t RHI/x$ by assuming that $\lambda_t RH/x$ is sufficiently large. It is assumed that, by repositioning vehicles, the number of vehicles at each parking station is rebalanced at intervals of duration H. The cost of repositioning is shown to be proportional to $H^{-1/2}$ but independent of the decision variables x, y, and m considered in this paper (See Section 7.2.2.1 in Daganzo and Ouyang (2019b)). Thus, the repositioning cost is omitted from the cost-minimizing objective function because the repositioning cost is constant if H is assumed to be given.

When passenger demand is high, the fleet size of idle vehicles at each parking station will be at a minimum because most vehicles will be on the road serving passenger demand. In such circumstances, there must be at least a certain number of parked vehicles to guarantee the level-of-service, preventing long waiting times for passengers and assignment failures. We have already set a confidence level p to ensure vehicle assignment from the nearest parking station in Equation 3.7. Using p, the required parking spaces per parking station $z^{req}(t)$ is formulated as follows:

$$z^{req}(t) = \Phi^{-1}(p)\sqrt{\frac{2\lambda_t RHI}{x}}, \tag{3.11}$$

where Φ is the standard normal distribution. The required density of parking spaces in the target region at demand λ_t is as follows:

$$y^{req}(t) = \frac{x \cdot z^{req}(t)}{R} = \Phi^{-1}(p)\sqrt{\frac{2\lambda_t HIx}{R}}. \tag{3.12}$$

As a result, the required fleet size in state P is formulated as:

$$n_P^{req}(t) = y^{req}(t)R = \Phi^{-1}(p)\sqrt{2\lambda_t RHIx}. \tag{3.13}$$

Finally, the density of parking station x can be expressed with respect to $T_{A,t}^1$. If the parking stations are uniformly distributed, the expected value of the distance between random demand to the nearest parking station, denoted by $d(x)$, is:

$$\begin{aligned} &E[d(x)] = T_{A,t}^1 v \\ &E[d(x)] \approx \frac{\kappa}{\sqrt{x}} \end{aligned}, \tag{3.14}$$

where the first expression is given by the definition of $T_{A,t}$ and the second expression is referenced from Daganzo and Ouyang (2019b). As a result, $T^1_{A,t}$ is expressed as a function of the decision variable x and vice versa: As a result,

$$
\begin{aligned}
T^1_{A,t} &= \frac{\kappa}{v_t\sqrt{x}},\\
x &= \frac{\kappa^2}{(v_t)^2}\cdot\frac{1}{(T^1_{A,t})^2}
\end{aligned}
\tag{3.15}
$$

According to Equations 3.6, 3.8, 3.9, and 3.13, the number of fleets in each state increases as the passenger demand (λ_t) increases. We reasonably assume that the average ground speed at the maximum demand, $v_{t_{\lambda_{max}}}$ is the slowest of the day, i.e., $v_{t_{\lambda_{max}}} = v_{min}$. Similarly, we assume that the average ground speed at the minimum demand, $v_{t_{\lambda_{min}}}$ is the fastest of the day, i.e., $v_{t_{\lambda_{min}}} = v_{max}$. Thus, the numbers of vehicles in states A, S, C, and P are the highest during the peak time:

$$
\begin{aligned}
&\left(n^{req}_A(t_{\lambda_{max}}) = \right)\lambda_{max}\frac{\kappa R}{v_{min}\sqrt{x}}(p+\alpha p-\alpha p^2) \geq \lambda_t\frac{\kappa R}{v_t\sqrt{x}}(p+\alpha p-\alpha p^2)\left(= n^{req}_A(t)\right),\\
&\left(n^{req}_S(t_{\lambda_{max}}) = \right)\lambda_{max}\frac{l_{t_{\lambda_{max}}}}{v_{min}} \geq \lambda_t\frac{l_t}{v_t}\left(= n^{req}_S(t)\right),\\
&\left(n^{req}_C(t_{\lambda_{max}}) = \right)\lambda_{max}\frac{\kappa R}{v_{min}\sqrt{x}}(q+\alpha q-\alpha q^2) \geq \lambda_t\frac{\kappa R}{v_t\sqrt{x}}(q+\alpha q-\alpha q^2)\left(= n^{req}_C(t)\right),\\
&\left(n^{req}_P(t_{\lambda_{max}}) = \right)\Phi^{-1}(p)\sqrt{2\lambda_{max}RHIx} \geq \lambda_t\Phi^{-1}(p)\sqrt{2\lambda_t RHIx}\left(= n^{req}_P(t)\right), \forall t.
\end{aligned}
\tag{3.16}
$$

Therefore, the minimum required fleet size m^* equals the required fleet size in $t_{\lambda_{max}}$ according to Equation 3.5, i.e., $\arg\max_t\,(m^{req}(t)) = t_{\lambda_{max}}$

When the demand rate is the lowest in $t_{\lambda_{min}}$, the highest number of idle vehicles are parked, so the confidence level p (the probability that there is at least one idle vehicle at the station nearest to a demand) can be set to 1 for further efficiency. On the other hand, during the peak hour $t_{\lambda_{max}}$, the confidence level q can be reasonably assumed to be 1 in the time window $t_{\lambda_{max}}$. Based on this, it is possible to simplify and rewrite the equations of m^* by using the maximum passenger demand (λ_{max}) , as follows:

$$
m^* = \lambda_{max}R\left(\frac{l_{t_{\lambda_{max}}}}{v_{min}}\right) + \lambda_{max}RT^1_{A,t_{\lambda_{max}}}(1+p+\alpha p-\alpha p^2) + \kappa\Phi^{-1}(p)\sqrt{2\lambda_{max}RHI}\frac{1}{v_{min}T^1_{A,t_{\lambda_{max}}}} \quad , \tag{3.17}
$$

Based on the operation depicted in Figure 1, extra vehicles beyond the required fleet sizes for states A, S, and C are not needed. In other words:

$$
n_A(t) = n^{req}_A(t), n_S(t) = n^{req}_S(t), n_C(t) = n^{req}_C(t), \forall t, \tag{3.18}
$$

On the other hand, as shown in Figure 3, the number of vehicles parked at parking stations in t, $n_P(t)$, is not always the same as $n^{req}_P(t)$, but can be found as Equation 3.19.

$$
n_P(t) = m^* - \big(n_A(t) + n_S(t) + n_C(t)\big), \tag{3.19}
$$

The number of vehicles not parked in stations, $n_A(t)+n_S(t)+n_C(t)$, is the lowest in $t_{\lambda_{min}}$, so the number of parked vehicles is the highest in $t_{\lambda_{min}}$. The minimum required number of parking spaces y^*R is the summation of the daily maximum number of required parking spaces, i.e., $n_P(t_{\lambda_{min}})$, and additional buffer spaces to guarantee that each parking station is not full by confidence level q, $\Phi^{-1}(q)\sqrt{2\lambda_{min}RHIx}$. As a result, the optimal density of parking spaces can be found as shown in Equation 3.20

$$
\begin{aligned}
y^* =& \frac{m^* - \left(n_A(t_{\lambda_{min}}) + n_S(t_{\lambda_{min}}) + n_C(t_{\lambda_{min}})\right) + \Phi^{-1}(q)\sqrt{2\lambda_{min}RHIx}}{R} \\
=& \left(\frac{\lambda_{max} l_{t_{\lambda_{max}}}}{v_{min}} - \frac{\lambda_{min} l_{t_{\lambda_{min}}}}{v_{max}}\right) \\
&+ \left((1+p+\alpha p-\alpha p^2)\lambda_{max} - (1+q+\alpha q-\alpha q^2)\lambda_{min}\cdot\frac{v_{min}}{v_{max}}\right) T^1_{A,t_{\lambda_{max}}} \\
&+ \frac{\kappa}{v_{min}}\left(\Phi^{-1}(p)\sqrt{\frac{2\lambda_{max}HI}{R}} + \frac{v_{min}}{v_{max}}\Phi^{-1}(q)\sqrt{\frac{2\lambda_{min}HI}{R}}\right)\left(\frac{1}{T^1_{A,t_{\lambda_{max}}}}\right)
\end{aligned}
. \tag{3.20}
$$

3.3. Solution of Optimal Parking Planning

The objective function in Equation 3.2 is reformulated in terms of $T^1_{A,t_{\lambda_{max}}}$ in Equation 3.21, which is a function of the remaining sole decision variable x (see $T^1_{A,t} = \frac{\kappa}{v_t\sqrt{x}}$ from Equation 3.15). There are four terms in Equation 3.21: the constant term, $\frac{1}{(T^1_{A,t_{\lambda_{max}}})^2}$, $\frac{1}{T^1_{A,t_{\lambda_{max}}}}$, and $T^1_{A,t_{\lambda_{max}}}$.

$$
\begin{aligned}
\min_{T_A} & \left(
\begin{aligned}
&\left((C_y + C_m)\left(\frac{\lambda_{max} l_{t_{\lambda_{max}}}}{v_{min}}\right) R - C_y\left(\frac{\lambda_{min} l_{t_{\lambda_{min}}}}{v_{max}}\right) R\right) \\
&+ \frac{C_x \kappa^2 R}{(v_{min})^2}\frac{1}{(T^1_{A,t_{\lambda_{max}}})^2} \\
&+ \left(\frac{\kappa(C_y + C_m)}{v_{min}}\Phi^{-1}(p)\sqrt{2\lambda_{max}HIR} + \frac{\kappa C_y}{v_{max}}\Phi^{-1}(q)\sqrt{2\lambda_{min}HIR}\right)\frac{1}{T^1_{A,t_{\lambda_{max}}}} \\
&+ \left((C_y + C_m)\lambda_{max}R(1+p+\alpha p-\alpha p^2) - C_y\lambda_{min}R(1+q+\alpha q-\alpha q^2)\frac{v_{min}}{v_{max}}\right) T^1_{A,t_{\lambda_{max}}}
\end{aligned}
\right) \\
s.t.\, & T_{A,t_{\lambda_{max}}} = T^1_{A,t_{\lambda_{max}}}(1+p+\alpha p-\alpha p^2) \le T_0,
\end{aligned}
\tag{3.21}
$$

For simplicity of derivation, each coefficient in Equation 3.21 are parameterized as P_0, P_{-2}, P_{-1}, and P_1 as shown in Equation 3.22.

$$
\min_{T^1_{A,t_{\lambda_{max}}}} Cost\left(T^1_{A,t_{\lambda_{max}}}\right) = \min_{T^1_{A,t_{\lambda_{max}}}} \left(P_0 + P_{-2}\frac{1}{(T^1_{A,t_{\lambda_{max}}})^2} + P_{-1}\frac{1}{T^1_{A,t_{\lambda_{max}}}} + P_1 T^1_{A,t_{\lambda_{max}}}\right), \tag{3.22}
$$

Since $\lambda_{max} > \lambda_{min}$ and all parameters are positive by definition, $P_0, P_{-2}, P_{-1}, P_1 > 0$. Therefore, Equation 3.22 is a convex curve in the first quadrant, and has a local minimum point in the first quadrant. Consequently, we take the derivative of Equation 3.22 to find the unconstrained optimal point.

$$
\begin{aligned}
&\frac{dCost\left(T^{1}_{A,t_{\lambda_{max}}}\right)}{dT^{1}_{A,t_{\lambda_{max}}}} = -2P_{-2}(T^{1}_{A,t_{\lambda_{max}}})^{-3} - P_{-1}(T^{1}_{A,t_{\lambda_{max}}})^{-2} + P_{1} = 0 \\
&-2P_{-2} - P_{-1}\left(T^{1}_{A,t_{\lambda_{max}}}\right) + P_{1}\left(T^{1}_{A,t_{\lambda_{max}}}\right)^{3} = 0 \\
&\left(T^{1}_{A,t_{\lambda_{max}}}\right)^{3} - \frac{P_{-1}}{P_{1}}T^{1}_{A,t_{\lambda_{max}}} - \frac{2P_{-2}}{P_{1}} = 0
\end{aligned}, \tag{3.23}
$$

For simplicity in derivation, let $A = \left(-\frac{P_{-1}}{P_{1}}\right)$ and $B = \left(-\frac{2P_{-2}}{P_{1}}\right)$. With realistic ranges of parameters, the discriminant (Δ) of the cubic equation is positive, and there are three distinct real roots as shown in Equation 3.24:

$$
\Delta = -\left(4A^{3} + 27B^{2}\right) > 0, \tag{3.24}
$$

When there are three real roots in cubic equation, François Viète (1540-1603) derived the trigonometric solution. The three real roots (t_k) can be calculated as shown in Equation 3.25:

$$
\begin{aligned}
&t^{3} + pt + q = 0 \\
&t_{k} = 2\sqrt{-\frac{p}{3}}\cos\left(\frac{1}{3}\arccos\left(\frac{3q}{2p}\sqrt{-\frac{3}{p}}\right) - k\frac{2\pi}{3}\right) \quad \text{for} \quad k = 0, 1, 2
\end{aligned}. \tag{3.25}
$$

The only positive solution is when $k = 0$. As a result,

$$
\begin{aligned}
T^{1,u}_{A,t_{\lambda_{max}}} &= 2\sqrt{-\frac{A}{3}}\cos\left(\frac{1}{3}\arccos\left(\frac{3B}{2A}\sqrt{\frac{-3}{A}}\right)\right) \\
&= 2\sqrt{\frac{P_{-1}}{3P_{1}}}\cos\left(\frac{1}{3}\arccos\left(\frac{6P_{-2}}{2P_{-1}}\sqrt{\frac{3P_{1}}{P_{-1}}}\right)\right)
\end{aligned}. \tag{3.26}
$$

Equation 3.26 is the unconstrained minimum of Equation 3.21. Thus, if $T_0 > (p + \alpha p - \alpha p^2)T^{1,u}_{A,t_{\lambda_{max}}}$, the constraint is not binding since $T_{A,t_{\lambda_{max}}} \geq T_{A,t}$, so that the optimal point $T^{1,*}_{A,t_{\lambda_{max}}} = T^{1,u}_{A,t_{\lambda_{max}}}$ and $Cost^{*} = Cost\left(T^{1,u}_{A,t_{\lambda_{max}}}\right)$. On the other hand, if $T_0 \leq (p + \alpha p - \alpha p^2)T^{1,u}_{A,t_{\lambda_{max}}}$, the constraint is binding, so that the optimal point $T^{1,*}_{A,t_{\lambda_{max}}} = \frac{T_0}{(p+\alpha p-\alpha p^2)}$ and $Cost^{*} = Cost\left(\frac{T_0}{(p+\alpha p-\alpha p^2)}\right)$:

$$
T^{1,*}_{A,t_{\lambda_{max}}} = \begin{cases} T^{1,u}_{A,t_{\lambda_{max}}}, & \text{if} \quad T_0 > (1 + p + \alpha p - \alpha p^2)T^{1,u}_{A,t_{\lambda_{max}}} \\ \frac{T_0}{(1+p+\alpha p-\alpha p^2)}, & \text{otherwise} \end{cases}. \tag{3.27}
$$

Then, based on the optimal decision variable ($T^{1,*}_{A,t_{\lambda_{max}}}$), we can calculate three parking operational variables (x, m, and y) by using Equation 3.15, Equation 3.17, and Equation 3.20, respectively. Since we have the analytical form of the solution, we can calculate parking operational variables in one shot.

Table 1
Model parameters

Variable	Units	Value
R	[km^2]	605.24
l	[km]	16.4
v_{min}	[km/hr]	18.0
v_{max}	[km/hr]	40.0
H	[hr]	2
p	-	0.95
q	-	0.95
α	-	2
I	-	1
κ	-	0.5
T_0	[min]	1

3.4. Discussion on the Integration of Dynamic Ride-sharing

While the proposed models in this study did not incorporate pooling or dynamic ride-sharing (DRS), it is worth mentioning that the models we have developed can be extended to include these considerations. Pooling, which entails combining multiple passengers with similar routes into a single trip, is another important component in Shared Autonomous Vehicle (SAV) parking planning according to several previous studies. Fakhrmoosavi et al. (2022) investigated the implications of parking strategies for SAV fleets, particularly in response to the growing demand for ride-hailing services, and emphasized that parking prices could be strategically utilized to encourage riders to opt for shared rides, thereby mitigating traffic congestion related to parking searches. Additionally, Yan et al. (2020) conducted a microsimulation study assessing the performance of SAV fleets in the Minneapolis-Saint Paul area. They analyzed the impact of trip densities and parking restrictions, revealing that SAVs could accommodate up to 30 person-trips per day with a wait time of under 5 minutes. This, however, led to a 13% increase in vehicle-miles traveled (VMT). Interestingly, the incorporation of DRS resulted in a 17% reduction in SAV VMT, underscoring the significance of DRS in curbing the VMT.

Responding to the necessity for the incorporation of pooling or DRS in parking planning for SAVs, our model is designed to be adaptable, serving as a foundational structure to which pooling or DRS elements can be appended. The modularity of our model facilitates seamless integration with other frameworks, thereby effectively addressing the challenges of incorporating pooling or DRS. While the proposed models in this paper do not directly address DRS, they are compatible with and can be complemented by the framework proposed by Daganzo and Ouyang (2019a), which delves into the DRS integration.

The integration of the parking planning models and DRS is beyond the scope of this paper. Nonetheless, in Appendix B, we briefly illustrate how a simple integration between the Single-Zone Analytical Parking Planning Model, and the "Shared Taxi" modeling presented in Section 5 of Daganzo and Ouyang (2019a), can be achieved. This integration provides initial insights into the interaction between parking planning and dynamic ride-sharing.

4. Case Study for Single-Zone Analytical Parking Planning Model

In this section, we demonstrate S-APPM through a case study in Seoul, South Korea. Specifically, we will discuss changes in the density of parking stations and parking spaces as well as fleet size required to serve passenger demand when system is optimized. The demand distribution in Seoul is not spatially uniform, but the results, assuming uniformity, can give an upper bound of system efficiency, which is useful at the beginning of high-level planning. The next model, T-APPM, which will be elaborated in Section 5, can be easily extended to a general multi-zonal framework. To realistically account for the spatial demand heterogeneity with zonal-specific parking planning, advanced models can be used instead of S-APPM to provide the upper bound of the reality.

Table 1 shows the parameters used in this case study. The area of Seoul is approximately 605.2km^2. According to

Table 2
Corresponding decision variables in the current transportation system in Seoul

Variable	Unit	Value
x_{Seoul}	[stations/km^2]	524.06
y_{Seoul}	[spaces/km^2]	7,150.24
z_{Seoul}	[spaces/stations]	13.64
m_{Seoul}	[veh]	2,703,429

Table 3
Hourly average passenger demand in Seoul. The values are in $[veh/km^2/hr]$

Time Window	Passenger Demand by Personal Vehicle	Passenger Demand by All Modes
Overall	285.11	1720.03
AM peak (7-9 AM)	765.04	4518.16
PM peak (6-8 PM)	836.94	4042.69
Off peak	181.93	1207.95

the Seoul Travel Survey[1], the average trip length is 16.4km, and the minimum and maximum speeds are 18.0km/hr and 40.0km/hr, respectively. We consider discrete time windows, each of which has a length of two hours. Both confidence levels, to guarantee that there is at least one vehicle at each parking station (p) and that there is at least one parking space left at each parking station (q), are set at 0.95. We assume α, the incremental ratio of travel time, to be 2 based on the assumption that the target area is homogeneous. Finding the second-nearest parking station would be, at most, equivalent to finding the nearest parking station first and then finding the second-nearest parking station from there. This means that the incremental ratio between the travel time to the nearest parking station and the second-nearest parking station would be less than or equal to 2. To consider the most pessimistic case, we assume $\alpha = 2$ to ensure that the results would provide a conservative estimate. The mean-to-variance ratio (I) is set to 1 assuming that occurrences of O-D events follow a Poisson distribution. Finally, κ is set to 0.5 referenced from Daganzo and Ouyang (2019b).

It is worth investigating actual numbers for each decision variable in Seoul. According to the statistics on parking infrastructures in Seoul[2] in 2021, there are 317,181 parking stations and 4,327,614 parking spaces, including public parking stations, private parking stations, and residential parking stations. Therefore, as shown in Table 2, the density of parking stations in Seoul is 524.09 stations/km^2, and the density of parking spaces in Seoul is 7150.72 spaces/km^2. There are approximately 13.64 parking spaces at each parking station. Moreover, there are 3,157,361 registered passenger vehicles in Seoul, which means that there are 0.625 parking spaces for each vehicle.

Table 3 shows the average hourly unit passenger demand (in [veh/km^2/hr]) in Seoul according to the National Household Travel Survey (O-D Flow Survey) in Korea. This survey offers the average hourly flow from one district to another, classified by mode of transportation and purpose of trip. The mode of transportation in this survey includes passenger vehicles, buses, subways, high-speed rail, walking, and bicycles; we extracted passenger demand by personal vehicle and passenger demand by all modes in the different time windows. Table 3 shows the corresponding values in each time window. The values in the total row represent the average passenger demand during any time-of-day. The values in the *Overall* row represent the average passenger demand throughout the day regardless of time-of-day. The values in the *AM peak* row represent the average passenger demand during the morning peak (7-9 AM); the values in *PM peak* row represent the average passenger demand during the afternoon peak (6-8 PM). In this study, we assume that passenger demand in time windows other than AM and PM peaks is equal to off-peak passenger demand. As a result, the values in the *Off-peak* row were calculated based on the values in the Overall, AM peak, and PM peak

[1] https://www.ktdb.go.kr/eng/index.do
[2] https://news.seoul.go.kr/traffic/archives/314

Table 4
Range of cost variables used in the sensitivity analysis.

Cost	Value	Reference
C_m	$[30, 31, \cdots, \mathbf{35.616}, \cdots, \mathbf{183.36}, \cdots, 200]$	Estrada et al. (2021)
C_x	$[0.1, 0.2, \cdots, 4.9, 5.0]$	-
C_y	$[0.1, 0, 2, \cdots, \mathbf{4.73}, \cdots, 20]$	Korean Ministry of Land, Infrastructure, and Transport

rows (i.e., we calculate the total demand for one day and subtract the AM peak and PM peak demands to get the Off-peak demand). Recent studies have shown that the demand for SAVs is expected to increase over time (Jones and Leibowicz, 2019; Narayanan et al., 2020a). In our model, we consider two demand types: "Passenger Demand by Personal Vehicle" and "Passenger Demand by All Modes." The primary purpose of this distinction is to emphasize the potential reduction in required parking spaces when comparing traditional vehicle usage to a fully implemented SAV system. While we acknowledge that the demand for SAVs will grow gradually over time, it is crucial for urban planning to look ahead and prepare for the long-term impact of such systems. By considering both demand types, our model highlights the potential benefits of SAV deployment in reducing parking requirements and underscores the importance of forward-thinking planning strategies to accommodate the anticipated growth in SAV demand.

In this case study, we analyze the results of our proposed model depending on different values for three operational costs: C_m, C_x, and C_y. The values and the references used for the sensitivity analysis are shown in Table 4. The daily operation cost of each SAV fleet (C_m) is referenced from Estrada et al. (2021), which analyzed the operational cost of the on-demand bus and taxi service, presenting the operational cost for different types of the powertrain (diesel and electric) and different sizes of vehicle (standard bus, mini-bus, and passenger car). In this study, we assume that each vehicle serves one passenger demand for one operation and SAVs use an electric powertrain; we use the *electric passenger car* as a reference vehicle for our study. In Estrada et al. (2021) there are two reference values without (35.616) and with (183.36) driver expenses. The value without driver expenses does not necessarily represent the cost of SAV fleets. Instead, we used it as a benchmark value while setting the range of C_m. Based on previous literature, such as Pakusch et al. (2020), labor costs usually take around 55% to 65% of the total operating cost of human-operated taxis. If human drivers are replaced by automated driving, the total operating cost of mobility service is expected to be reduced. However, we cannot make any reasonable assumptions about how the cost will be for SAV fleets. As a result, we set the range of C_m from 30 to 200 \$/veh/day. The daily operation cost of the parking station (C_x) includes costs, such as amortized installation cost of the parking management system in the parking station. The daily operation cost of parking spaces (C_y) includes the amortized cost of purchasing the land used for the parking spaces and the construction cost for parking spaces. There are not many references to support our reasoning for choosing an appropriate value for C_x, but C_x must be smaller than or similar to C_y because the installation cost of the parking management system is not expensive compared to the overall land price for the parking spaces. We referenced one value for C_y from the *declared land value* announced by the Korean Ministry of Land, Infrastructure, and Transport. The average land price in Seoul is 2490.35 $\$/\text{m}^2$, and the average area of each parking space is 3.3 m^2. We assume that the land price is equivalent to a five-year rental cost with 2% annual interest rate. As a result, the amortized daily cost for each parking space is $\left(\frac{2490.35 \cdot 3.3 \cdot \frac{0.02}{365}}{1-\left(1+\frac{0.02}{365}\right)^{-365 \cdot 5}}\right) = 4.73\$/spaces/day$ considering only the land price. We set the range of C_y from 0.1 to 20 $\$/spaces/day$ for the sensitivity analysis Finally, since C_x should be similar to or less than C_y, we set the range of C_x from 0.0 to 5.0 $\$/stations/day$.

Figure 4 and Figure 5 show the results of sensitivity analysis. The passenger demand by personal vehicle in Table 3 is used for the sensitivity analysis. Figure 4 shows the result with different C_m and C_y when C_x is fixed to $2\$/stations/day$. Figure 5 shows the result with different C_x and C_y when C_m is fixed to $35.616\$/veh/day$. There are six results of different variables in each figure: Total cost in million USD ($Cost$), Passenger waiting time ($T_A = T^1_{A,t_{\lambda_{max}}}(p + \alpha p - \alpha p^2)$) in minutes, the number of SAV fleets (m), density of parking stations (x), density of parking spaces (y), and the average number of parking spaces in each parking station (z).

Figure 4 (a) shows that the total cost significantly drops as C_m decreases. This result shows that replacing human-driven taxis with SAVs will significantly improve cost-efficiency. In Figure 4 (b), when C_m is fixed, there is an increas-

Table 5
Summary of results of Case Study for S-APPM

Demand	Variable		Current	Optimal	
Personal Vehicle	x	[stations/km^2]	524.09	11.66	(-97.75%)
	y	[spaces/km^2]	7,150.72	718.22	(-89.96%)
	z	[spaces/station]	13.64	61.59	($+351.54\%$)
	m	[veh]	2,703,429	477,944.71	(-82.32%)
	yR/m	[spaces/veh]	1.601	0.9095	(-43.19%)
All Mode	x	[stations/km^2]	524.09	27.51	(-94.75%)
	y	[spaces/km^2]	7,150.72	3728.66	(-47.86%)
	z	[spaces/station]	13.64	135.52	($+893.55\%$)
	m	[veh]	2,703,429	2,549,647.66	(-5.69%)
	yR/m	[spaces/veh]	1.601	0.8851	(-44.72%)

ing tendency in T_A as C_y increases. On the other hand, there is a decreasing tendency in T_A as C_m increases when C_y is fixed. Within the realistic range of each cost value, the unconstrained minimum of Equation 3.22 ($T^{1,u}_{A,t_{\lambda_{max}}}$) is not bounded by the constraint, $T_0 \leq (p + \alpha p - \alpha p^2)T^{1,u}_{A,t_{\lambda_{max}}}$, so the optimal value for $T^{1}_{A,t_{\lambda_{max}}}$ is equal to $T^{1,u}_{A,t_{\lambda_{max}}}$. As a result, three operational variables can be calculated from the derived Equations in Section 3.2.

The number of SAV fleets (m) is calculated based on Equation 3.17; the results are shown in Figure 4 (c). Similar to T_A, there is an increasing tendency in m as C_y increases and there is a decreasing tendency in m as C_m increases. Furthermore, the density of parking spaces (x) is proportional to the square of reciprocal of T_A as shown in Equation 3.15. As a result, there is a decreasing tendency in x as C_y increases and there is an increasing tendency in x as C_m increases as shown in Figure 4 (d). Within the range of T_A shown in Figure 4 (a), the T_A term in Equation 3.20 is relatively smaller than $\frac{1}{T_A}$ term. As a result, y has a tendency opposite to T_A as shown in Figure 4 (e).

Figure 5 (a) shows the change in total cost with different values of C_x and C_y; the overall cost decreases as C_y decreases. In Figure 5 (b), when C_x is fixed, there is an increasing tendency in T_A as C_y increases. Similarly, as C_x increases, there is an increasing tendency in T_A. When the cost of parking facilities is low, it is relatively cost-efficient to install more parking stations and parking spaces. The passenger waiting time consequently decreases as the number of parking stations increases. Similar to the previous results in Figure 4, m follows a similar tendency with T_A, while x and y follow a tendency opposite to that of T_A.

Table 5 shows a summary of the results for different levels of demand. The upper part of the table shows the results when SAVs serve current passenger demand for personal vehicles; the lower part shows the results when SAVs serve passenger demand for all modes, including private vehicles and public transportation. To derive these results, we used $C_m = 35.616$ to show that all vehicles are autonomous vehicles without human drivers, and $C_y = 4.73$ to represent the land price in Seoul. $C_x = 2$ was arbitrarily chosen.

The values in the column named "Current" show the values corresponding to the current transportation system in Seoul; the values in the column marked "Optimal" show results of S-APPM when the SAV system replaces the current transportation system. The results show that it is possible to significantly decrease the number of parking stations, parking spaces, and vehicles by introducing the SAV system. The density of parking stations decreases 97.75% and the density of parking spaces for personal vehicle demand decreases 89.96%. It is notable that the average number of parking spaces at each parking station (z) increases from 13.64 to 61.59. The current system in Seoul has fewer parking spaces in one parking station and the parking stations are dense. However, the optimal solution for the SAV system suggests that sparse parking stations with more parking spaces at each station will be more cost-efficient. The fleet size (m) also significantly decreases. Approximately 5.66 personal vehicles can be replaced with one SAV. Finally, the number of parking spaces for each vehicle decreases from 1.601 to 0.9095. There is less than one parking space for one vehicle in the optimal solution. This means that at least 9.05% of vehicles are out on the road serving passengers. This is because of the demand setting. The passenger demand at off-peak is assumed to be the same at any time window other than those at AM-peak and PM-peak. With better data on passenger demand, this result can realistically be improved.

When passenger demand increases to the demand by all mode, as shown in Table 5, all three operational variables increase corresponding to the increase in demand. Although the density of parking stations increased, the density of parking spaces increased more significantly. As a result, the average number of parking spaces at each parking station (z) increased too. This again shows that sparse parking stations with more parking spaces at each station will be more cost-efficient.

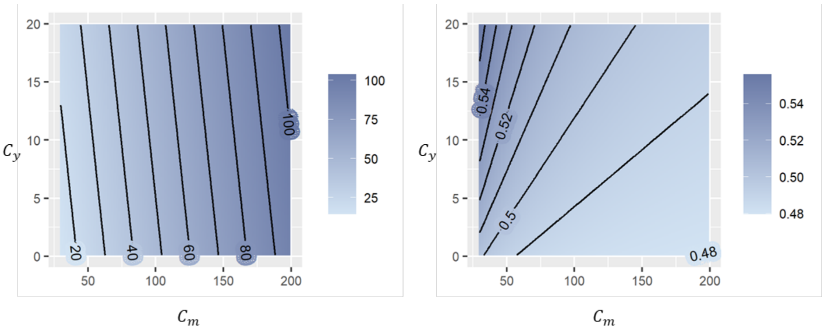

(a) Total *Cost* in million USD (b) Passenger waiting time (T_a)

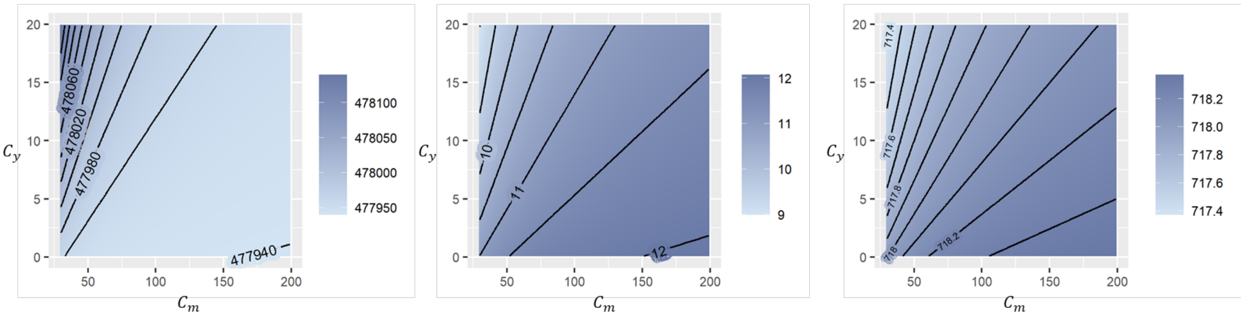

(c) The number of SAV fleets (m) (d) Density of parking stations (x) (e) Density of parking stations (y)

Figure 4: Result of the sensitivity analysis between C_m and C_y, when $C_x = 2\$/stations/day$

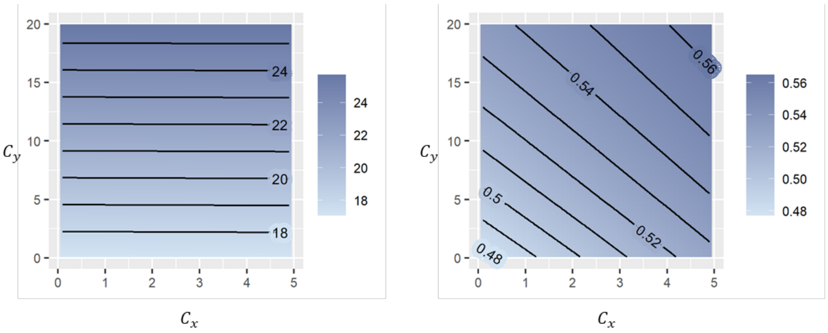

(a) Total *Cost* in million USD (b) Passenger waiting time (T_a)

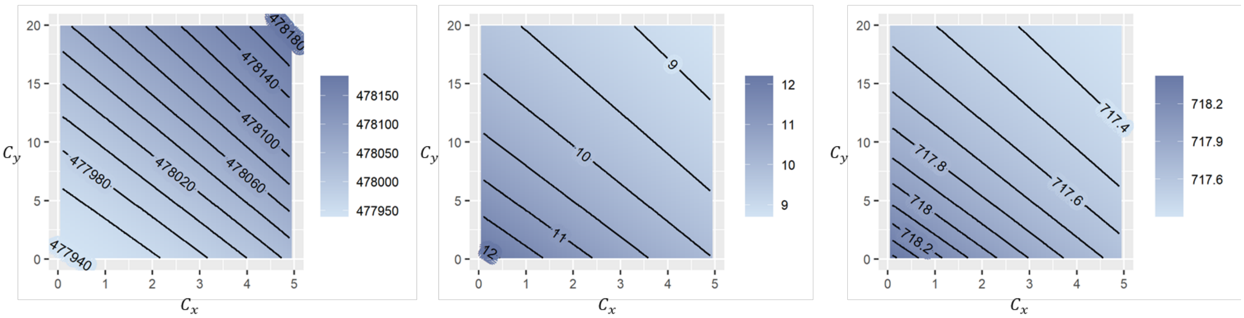

(c) The number of SAV fleets (m) (d) Density of parking stations (x) (e) Density of parking stations (y)

Figure 5: Results of sensitivity analysis between C_x and C_y, when $C_m = 35.616\$/spaces/day$

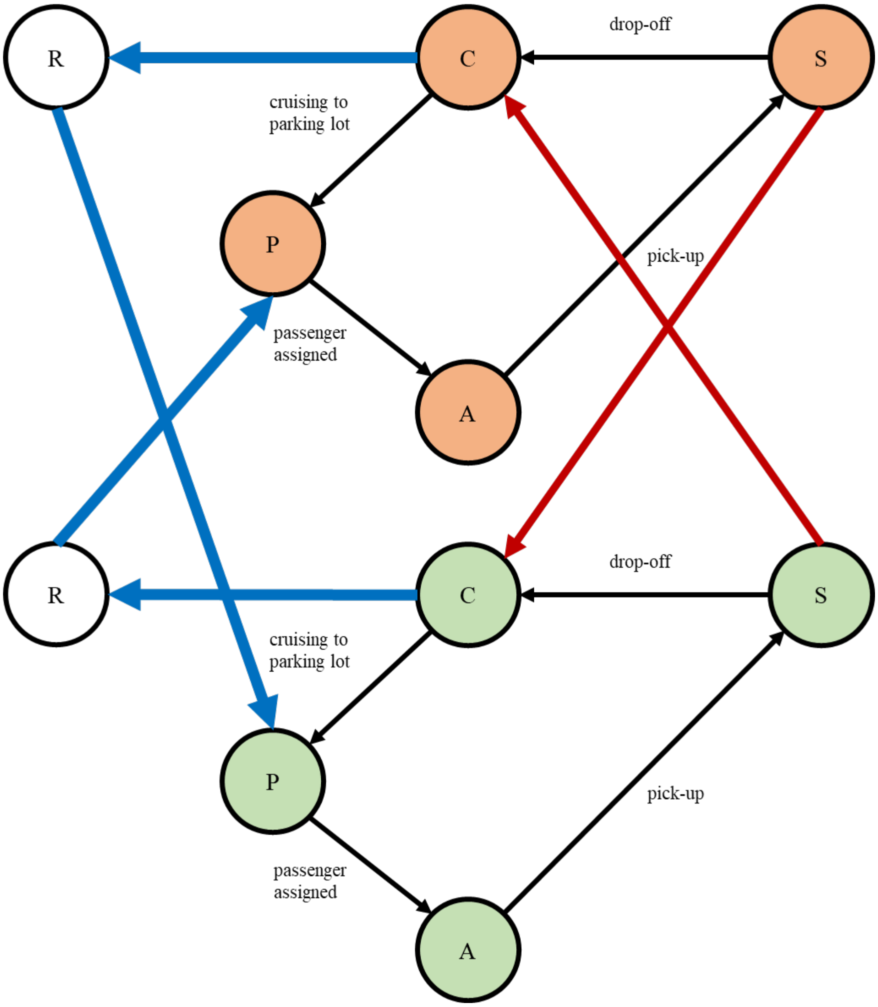

Figure 6: Workload representation of Two-zone Analytical Parking Planning Model (T-APPM)

5. Two-Zone Analytical Parking Planning Model

In this section, we model the *Two-zone Analytical Parking Planning Model (T-APPM)* by extending S-APPM, as shown in Figure 6. Since T-APPM considers the target region as two distinguishable zones, the model must consider inter-zonal movements. First, the origin and destination of passenger trips can be located in different zones. The red lines in Figure 6 indicate passenger trips from one zone to another. Second, it is necessary to consider relocation of SAVs. When the passenger demand is higher in one direction than the opposite, the number of SAV fleets (both parked and running) in one zone will continuously increase. For example, in the morning peak, passenger demand from suburb to city center will be much higher than passenger demand from city center to suburb. When this demand pattern continues, there will be more vehicles in the city center and fewer vehicles in the suburb, causing a lack of parking spaces in the city center and a decrease in level-of-service in the suburb by increasing the passenger waiting time. As a result, a proper relocation strategy for SAVs should be considered. The blue lines in Figure 6 describes the flow of vehicles that are relocated to the other zone after finishing passenger trips.

Figure 7 shows an example of T-APPM. A passenger calls for a trip from a suburb (colored in green) to the city center (colored in orange). The black line in Figure 7 (b) represents the movement of the assigned vehicle from the parking station to the passenger's origin. This corresponds to the state transition from P to A and the state transition from A to S in S-APPM of the suburb zone. The red line in Figure 7 (b) represents the passenger trip from the suburb to the city center, which corresponds to the state transition from S in the suburb to C in the city center. Then, this

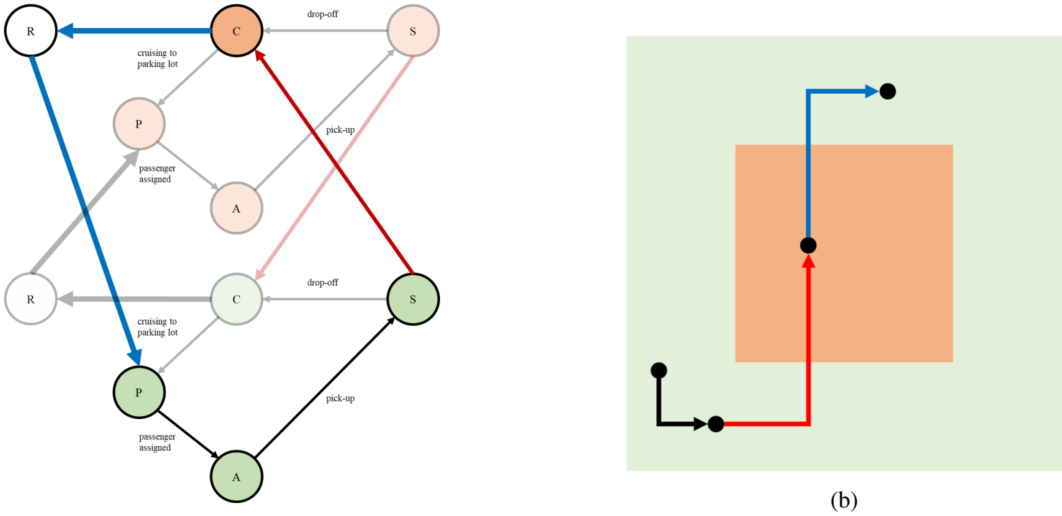

(a) (b)

Figure 7: Example case of T-APPM. Black line represents the vehicle traveling from the parking station to passenger's origin, red line represents the passenger trip, and blue line represents the relocation of the vehicle.

vehicle is relocated to the suburb, which is represented by the blue line in Figure 7 (b). This corresponds to the state transition from C in the city center to R (relocation state), and the state transition from R to P in the suburb.

Consider a given target region divided into two separate zones, as shown in Figure 7 (b). The inner zone (zone 1) colored in orange has a size of R_1; the outer zone (zone 2), colored in green has a size of R_2. In zone 1, the density of parking stations is denoted as x_1, and the density of parking spaces is denoted as y_1. Likewise, the density of parking stations in zone 2 is denoted as x_2 and the density of parking stations in zone 2 is denoted as y_2. The total number of SAV fleets is denoted as $M = m_1 + m_2$, where m_1 and m_2 represents the number of SAV fleets in zone 1 and zone 2, respectively. Similar to the assumptions in S-APPM, when passenger demand is generated, an SAV in the nearest not-empty parking station is assigned to the passenger ($P \rightarrow A$). This SAV cruises to the origin of the passenger and picks up the passenger ($A \rightarrow S$). The SAV travels from the origin to the destination and drops off the passenger ($S \rightarrow C$). If the SAV is relocated to a different zone ($C \rightarrow R$), the vehicle moves to the nearest parking station in the relocated zone ($R \rightarrow P$). Otherwise, the SAV moves to a parking station in the same zone from the destination of the passenger ($C \rightarrow P$)

5.1. Objective Function

The objective function of T-APPM is to minimize the total operation cost in the target regions: i) parking station operation costs in both zones, ii) parking space operation costs in both zones, and iii) fleet operation costs. The parking station operation cost (C_x) and fleet operation cost (C_m) are not different across two zones. However, the parking space operation cost (C_y) can be different across two zones because it includes the land cost. As a result, we assume that two zones have different cost values for C_y, but they have the same cost values for C_x and C_m. The objective function J is to minimize overall daily average operation cost ($Cost$) formulated as a function of the planning variables (x_1, x_2, y_1, y_2, M) with respect to LOS constraint:

$$J = \min_{x_1,x_2,y_1,y_2,M} Cost(x_1, x_2, y_1, y_2, M) = \min_{x_1,x_2,y_1,y_2,M} \Big(C_x(x_1 R_1 + x_2 R_2) + C_{y,1} y_1 R_1 + C_{y,2} y_2 R_2 + C_m M \Big), \quad \text{s.t.} T_{A,t} \le T_0 \tag{5.1}$$

where $C_{y,1}$ is the unit cost for each parking space in zone 1, and $C_{y,2}$ is the unit cost for each parking space in zone 2. x_1 and x_2 represent the density of parking stations in each zone, y_1 and y_2 represent the density of parking stations in each zone, and M represents the total number of SAV fleets for the operation. $T_{A,t}$ is the average passenger waiting time in time window indexed by t, and T_0 is the threshold, the maximum allowed average passenger waiting time.

5.2. SAV Operation Model with Parking and Relocation

For a given time window (t), we define a passenger demand matrix as $\mathbf{\Lambda}^t$ as follows:

$$\mathbf{\Lambda_t} = \begin{bmatrix} \lambda_{t,11} & \lambda_{t,12} \\ \lambda_{t,21} & \lambda_{t,22} \end{bmatrix}, \tag{5.2}$$

where $\lambda_{t,ij}$ refers to the unit passenger demand from zone i to zone j in the given time window t. It is assumed that the origin of passenger demand is uniformly distributed in zone i and the destination of passenger demand is uniformly distributed in zone j.

The total number of SAV fleets can be derived by summing the numbers of vehicles at all states. Similar to the derivations in Section 3, we first calculate the "required" number of SAV fleets by summing the required number of SAV fleets in each state to ensure the level-of-services as follows:

$$\begin{aligned} M^{req}(t) =& m_1^{req}(t) + m_2^{req}(t) \\ =& \left(n_{1,A}^{req}(t) + n_{1,S}^{req}(t) + n_{1,C}^{req}(t) + n_{1,P}^{req}(t) + n_{1,R}^{req}(t) \right) \\ &+ \left(n_{2,A}^{req}(t) + n_{2,S}^{req}(t) + n_{2,C}^{req}(t) + n_{2,P}^{req}(t) + n_{2,R}^{req}(t) \right) \end{aligned}, \tag{5.3}$$

where the first part(i) of the subscript of $n_{i,X}$ refers to the zone, and the second part(X) refers to the state of the vehicle. For example, $n_{2,P}$ refers to the number of SAV fleets in "Parked" state in Zone 2. Then, the number of SAV fleets (M^*) is the maximum of M^{req}

$$M^* = \max_t (M^{req}(t)) \tag{5.4}$$

The number of SAV in states A, S, C, and P can be calculated based on the derivations from S-APPM. First, we can calculate the number of vehicles in state A as shown in Equation 5.5.

$$\begin{aligned} n_{1,A}^{req}(t) &= (\lambda_{t,11} + \lambda_{t,12}) R_1 T_{A,t_1}^1 (p + \alpha p - \alpha p^2) \\ n_{2,A}^{req}(t) &= (\lambda_{t,22} + \lambda_{t,21}) R_2 T_{A,t_2}^1 (p + \alpha p - \alpha p^2) \end{aligned}. \tag{5.5}$$

where T_{A,t_1}^1 and T_{A,t_2}^1 are the average travel time from the nearest parking station to the origin of the passenger of two zones.

Second, the number of SAV in state S can be calculated as shown in Equation 5.6.

$$\begin{aligned} n_{1,S}^{req}(t) &= \lambda_{t,11} R_1 \left(\frac{l_{t,11}}{v_{t,11}} \right) + \lambda_{t,12} R_1 \left(\frac{l_{t,12}}{v_{t,12}} \right) \\ n_{2,S}^{req}(t) &= \lambda_{t,22} R_2 \left(\frac{l_{t,22}}{v_{t,22}} \right) + \lambda_{t,21} R_2 \left(\frac{l_{t,21}}{v_{t,21}} \right) \end{aligned}, \tag{5.6}$$

where $l_{t,ij}$ is the average trip length from zone i to zone j in time window t, and $v_{t,ij}$ is the average speed from zone i to zone j in time window t.

Third, the number of SAV fleets in state C can be calculated as shown in Equation 5.7:

$$\begin{aligned} n_{1,C}^{req}(t) &= (\lambda_{t,11} R_1 + \lambda_{t,21} R_2) T_{C,t_1}^1 (q + \alpha q - \alpha q^2) \\ n_{2,C}^{req}(t) &= (\lambda_{t,22} R_2 + \lambda_{t,12}) R_1 T_{C,t_2}^1 (q + \alpha q - \alpha q^2) \end{aligned}. \tag{5.7}$$

where $T_{C,t_1}^1 = T_{A,t_1}^1$ and $T_{C,t_1}^2 = T_{A,t_1}^2$.

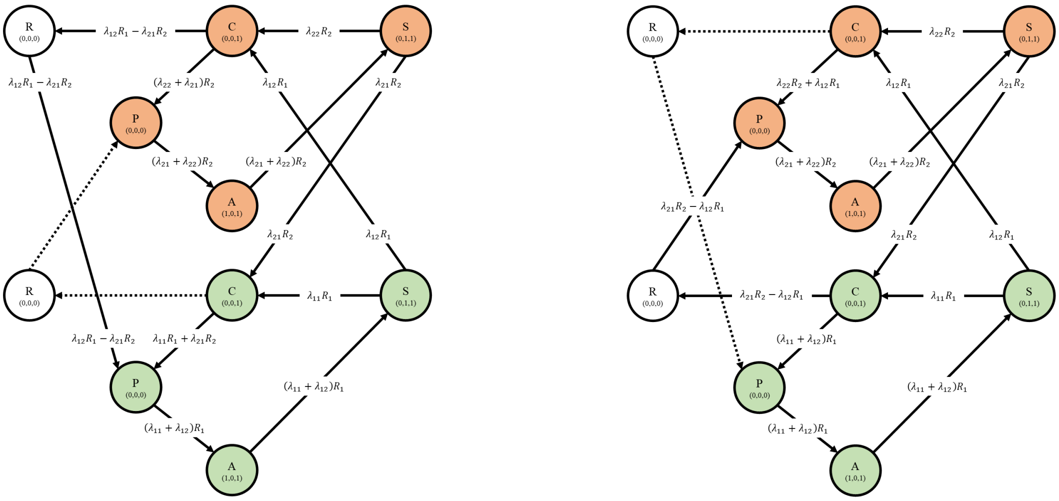

(a) $\lambda_{12}R_1 > \lambda_{21}R_2$ (b) $\lambda_{12}R_1 < \lambda_{21}R_2$

Figure 8: Graphical Illustration of the average flow in each state transition link in different demand condition

Next, the required number of SAV fleets in state P can be calculated as shown in Equation 5.8.

$$
\begin{aligned}
n^{req}_{1,P}(t) &= \Phi^{-1}(p)\sqrt{2(\lambda_{t,11} + \lambda_{t,12})R_1 H I x_1} \\
n^{req}_{2,P}(t) &= \Phi^{-1}(p)\sqrt{2(\lambda_{t,22} + \lambda_{t,21})R_2 H I x_2}
\end{aligned}, \tag{5.8}
$$

The formulations for deriving the number of SAV fleets in state R are different depending on the demand condition. If there is more passenger demand from zone 1 to zone 2 than there is from zone 2 to zone 1, there will be an increasing number of SAV fleets in zone 2. As a result, some vehicles should be relocated from zone 2 to zone 1. On the other hand, if there is more passenger demand from zone 2 to zone 1 than there is demand from zone 1 to zone 2, there will be an increasing number of SAV fleets in zone 1. In this case, relocation of vehicles should be from zone 1 to zone 2. Figure 8 shows the average flow in each state transition link in both cases.

As a result, if $\lambda_{12}R_1 > \lambda_{21}R_2$,

$$
\begin{aligned}
n^{req}_{1,R}(t) &= 0 \\
n^{req}_{2,R}(t) &= (\lambda_{t,12}R_1 - \lambda_{t,21}R_2)T_{R_{21}} = (\lambda_{t,12}R_1 - \lambda_{t,21}R_2)\frac{l_{21}}{v_{t,21}}
\end{aligned}, \tag{5.9}
$$

and if $\lambda_{21}R_2 > \lambda_{12}R_1$,

$$
\begin{aligned}
n^{req}_{1,R}(t) &= (\lambda_{t,21}R_2 - \lambda_{t,12}R_1)T_{R_{12}} = (\lambda_{t,21}R_2 - \lambda_{t,12}R_1)\frac{l_{12}}{v_{t,12}}, \\
n^{req}_{2,R}(t) &= 0
\end{aligned} \tag{5.10}
$$

where $T_{R_{ij}}$ refers to the average travel time of vehicles that are being relocated from zone i to zone j, and l_{ij} refers to the average trip length of vehicles that are being relocated from zone i to zone j.

$n^{req}_{1,R}(t)$ and $n^{req}_{2,R}(t)$ can have different values depending on passenger demand and parameter settings. Consequently, it is not feasible to find a closed-form solution for the optimal values of the operation variables. Thus, we ran a numerical analysis to find the optimal values. We first defined four time windows that maximized and minimized the required fleet size at each zone, as follows:

$$\begin{aligned} t_{1,max} &= \arg\max_t \left(m_1^{req}(t)\right), \\ t_{2,max} &= \arg\max_t \left(m_2^{req}(t)\right), \\ t_{1,min} &= \arg\min_t \left(m_1^{req}(t)\right), \\ t_{2,min} &= \arg\min_t \left(m_2^{req}(t)\right), \end{aligned} \tag{5.11}$$

We assume that the average ground speeds within the same zone in the time windows, $v_{11,t_{1,max}}$, $v_{22,t_{2,max}}$, $v_{11,t_{1,min}}$, and ,$v_{22,t_{2,min}}$, are the slowest and fastest of the day in each zone, i.e., $v_{11,t_{11,max}} = v_{11,min}$, $v_{22,t_{22,max}} = v_{22,min}$, $v_{11,t_{11,min}} = v_{11,max}$, and $v_{22,t_{22,min}} = v_{22,max}$. Furthermore, we assume that the average speeds between two zones are constant: $v_{t,12} = v_{12}$ and $v_{t,21} = v_{21}$.

Then, we can rewrite the equations of the minimum required fleet size of each zone, m_1^* and m_2^* as follows:

$$\begin{aligned} m_1^* &= m_1^{req}(t_{1,max}) \\ m_2^* &= m_2^{req}(t_{2,max}) \end{aligned} \tag{5.12}$$

Based on the operation depicted in Figure 7b, extra vehicles on the top of required fleet sizes for states A, S, C, and R are not needed. In other words:

$$\begin{aligned} n_{1,A}(t) &= n_{1,A}^{req}(t), n_{1,S}(t) = n_{1,S}^{req}(t), n_{1,C}(t) = n_{1,C}^{req}(t), n_{1,R}(t) = n_{1,R}^{req}(t) \\ n_{2,A}(t) &= n_{2,A}^{req}(t), n_{2,S}(t) = n_{2,S}^{req}(t), n_{2,C}(t) = n_{2,C}^{req}(t), n_{2,R}(t) = n_{2,R}^{req}(t) \end{aligned} \tag{5.13}$$

On the other hand, the number of vehicles parked at parking stations in t, $n_P(t)$, is not always the same as $n_P^{req}(t)$, but can be found as Equation 5.14:

$$\begin{aligned} n_{1,P}(t) &= m_1^* - \left(n_{1,A}(t) + n_{1,S}(t) + n_{1,C}(t) + n_{1,R}(t)\right) \\ n_{2,P}(t) &= m_2^* - \left(n_{2,A}(t) + n_{2,S}(t) + n_{2,C}(t) + n_{2,R}(t)\right) \end{aligned} \tag{5.14}$$

The number of vehicles not parked in stations in zone i, $n_{i,A}(t) + n_{i,S}(t) + n_{i,C}(t) + n_{i,R}(t)$, is the lowest in $t_{i,min}$, so the number of parked vehicles is the highest in $t_{i,min}$. The minimum required number of parking spaces in zone i, $y_i R_i$, is the summation of the daily maximum number of required parking spaces, i.e., $n_P(t_{i,min})$ and additional buffer spaces to guarantee that each parking station is not full by confidence level q. As a result, the optimal density of parking spaces can be found as shown in Equation 5.15

$$\begin{aligned} y_1^* &= \frac{m_1^* - \left(n_{1,A}(t_{1,min}) + n_{1,S}(t_{1,min}) + n_{1,C}(t_{1,min}) + n_{1,R}(t_{1,min})\right) + \Phi^{-1}(q)\sqrt{2\left(\lambda_{t,11}R_1 + \lambda_{t,21}R_2\right) HIx_1}}{R_1} \\ y_2^* &= \frac{m_2^* - \left(n_{2,A}(t_{2,min}) + n_{2,S}(t_{2,min}) + n_{2,C}(t_{2,min}) + n_{2,R}(t_{1,min})\right) + \Phi^{-1}(q)\sqrt{2\left(\lambda_{t,22}R_2 + \lambda_{t,12}R_1\right) HIx_2}}{R_2} \end{aligned} \tag{5.15}$$

The density of parking stations (x_i) can be calculated similar to Equation 3.15 as shown below:

$$\begin{aligned} x_1 &= \frac{\kappa^2}{\left(v_{t_{1,max},11}\right)^2} \cdot \frac{1}{\left(T^1_{A,t_{1,max}}\right)^2} \\ x_2 &= \frac{\kappa^2}{\left(v_{t_{2,max},22}\right)^2} \cdot \frac{1}{\left(T^1_{A,t_{2,max}}\right)^2} \end{aligned}, \tag{5.16}$$

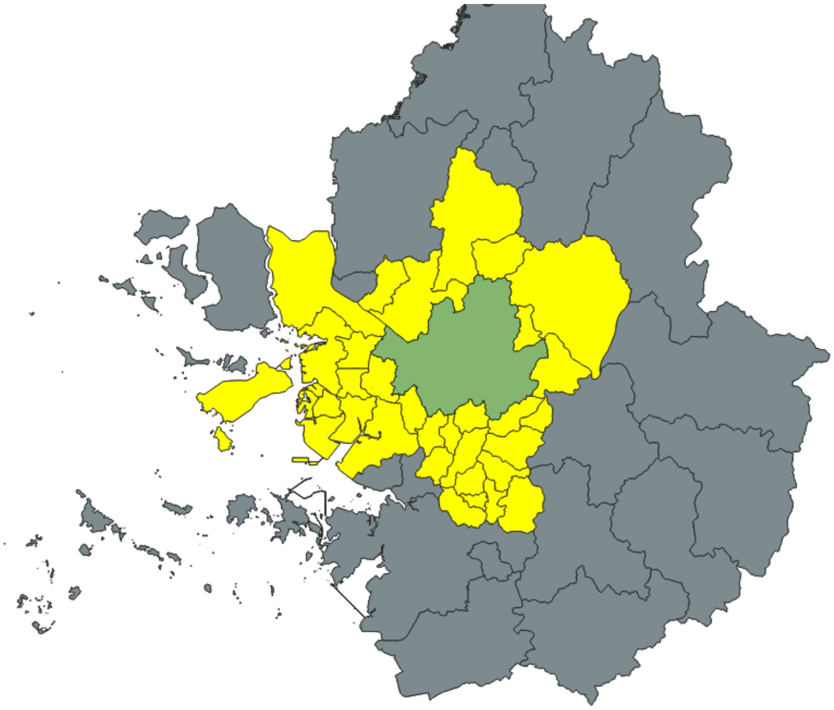

Figure 9: Map of Seoul Metropolitan Area. The green region represents Seoul city, while the yellow and gray regions represent Gyeonggi-do and Incheon city. Yellow regions are selected as the target region in Gyeonggi-do in this study.

The objective function in Equation 5.1 can be reformulated in terms of $T^1_{A,t_{1,max}}$ and $T^1_{A,t_{2,max}}$. We numerically find the optimal values for $T^1_{A,t_{1,max}}$ and $T^1_{A,t_{2,max}}$ that minimizes total operation cost.

6. Case Study for Two-Zone Analytical Parking Planning Model

In this section, we will extend the case study in Section 4 and discuss the findings for T-APPM. The main difference between S-APPM and T-APPM is that T-APPM considers inter-region passenger demand as well as the relocation of the SAV fleet. We extend the spatial range to the Seoul Metropolitan Area (i.e. Seoul Capital Area, or Sudogwon).

The Seoul Metropolitan Area refers to the metropolitan area near Seoul, including Seoul, Incheon, and Gyeonggi-do, located in the northwest part of South Korea. The population of this area is approximately 26 million people, more than half the population of South Korea. Figure 9 provides a map of the Seoul Metropolitan Area. The green region is Seoul city, while the yellow and gray regions are Gyeonggi-do and Incheon city. Gyeonggi-do and Incheon city cover a wide range of regions, as shown in Figure 9. As a result, if we consider the whole area as the target region for our case study, intra-region travel times and inter-region travel times will be too long. It would be inefficient and unrealistic for SAVs to travel long distances for relocation and passenger trips. Therefore, we select sub-regions near Seoul that have a relatively considerable number of passenger trips to Seoul. The selected area is colored in yellow in Figure 9; this region will be referred to as *Gyeonggi* for the rest of this case study.

Table 6 shows the average hourly unit passenger demand for our case study according to the Korean National Household Travel Survey (Origin-Destination Flow Survey). Similar to Table 3, the table shows corresponding values for each time window. Unit passenger demand is calculated based on origin. For example, if there were 52,982.71 passengers traveling from Seoul to Gyeonggi, we divided the number of passengers by the area of the origin zone, and the result was 87.54 $[veh/km^2/hr]$. Similar to Table 3, the values in the total row represent average passenger demand during any time-of-day. The values in the *AM peak* row represent average passenger demand during the morning peak (7-9 AM), and the values in the *PM peak* row represent average passenger demand during the afternoon peak (6-8

Table 6
Hourly average passenger demand in Seoul. The unit of the values is $[veh/km^2/hr]$

Time	Origin	Destination	Passenger Demand by Personal Vehicle	Passenger Demand by All Mode
Overall	Seoul	Seoul	285.11	1720.03
	Seoul	Gyeonggi	87.54	191.06
	Gyeonggi	Seoul	18.90	40.80
	Gyeonggi	Gyeonggi	79.33	232.69
AM peak (7-9 AM)	Seoul	Seoul	765.04	4518.16
	Seoul	Gyeonggi	280.37	448.92
	Gyeonggi	Seoul	70.32	165.51
	Gyeonggi	Gyeonggi	216.07	619.37
PM peak (6-8 PM)	Seoul	Seoul	836.94	4042.69
	Seoul	Gyeonggi	340.25	795.70
	Gyeonggi	Seoul	58.01	85.71
	Gyeonggi	Gyeonggi	225.83	525.61
Off peak	Seoul	Seoul	181.93	1207.95
	Seoul	Gyeonggi	42.98	104.81
	Gyeonggi	Seoul	9.85	23.84
	Gyeonggi	Seoul	51.01	164.73

PM). In this study, we assume that passenger demand values in time windows other than AM and PM peaks are equal to off-peak passenger demand. As a result, the values in the *Off-peak* row were calculated based on the values in the Total, AM peak, and PM peak rows.

Table 7 shows the model parameters used for the case study. The area of Seoul is 605.24 km^2; the area of Gyeonggi (selected areas only) is 2799.20 km^2. l_{ij} represents the average travel distance from zone i to zone j. The passenger demand is assumed to be uniformly distributed, so l_{ij} is the average distance between one random point in zone i and one random point in zone j. We use the following approximation from Rodriguez-Bachiller (1983) and Wilson (1990) to calculate l_{ij}:

$$\begin{aligned} l_{ij} &= \sqrt{\left(\left(\bar{d}_{i*}\right)^2 + \left(\bar{d}_{j*}\right)^2\right) + \left(\bar{d}^*_{ij}\right)^2} \\ &\approx \sqrt{0.18\left(R_i + R_j\right) + \left(\bar{d}^*_{ij}\right)^2} \end{aligned}, \tag{6.1}$$

where $\bar{d}_{i*}$ is the average distance from one point in zone i to the centroid of zone i, and $\bar{d}^*_{ij}$ is the distance between the centroids of zone i and zone j. In the Table 7, the subscript s refers to Seoul and the subscript g refers to Gyeonggi. For example, l_{sg} refers to the average travel distance from Seoul to Gyeonggi.

Because we covered the sensitivity analysis of different cost values in Section 3, we assumed in this section that the costs are pre-determined. We used 35.36 $\$/veh/day$ for C_m referenced from Estrada et al. (2021).$C_{y,1}$ is assumed to be 4.73 $\$/spaces/day$ and $C_{y,2}$ is assumed to be 0.24 $\$/spaces/day$, which are the amortized land cost of two zones respectively, referenced from declared land value announced by the Korean Ministry of Land, Infrastructure, and Transport. We assumed that C_x is 1 $\$/stations/day$ to make sure that C x was neither too large nor too small compared to the other cost variables.

The results of this case study are shown in Table 8. To analyze the effect of relocation and inter-zonal demands in T-APPM, we compare the results of T-APPM with three baselines. The first baseline is the current operating values in Seoul and Gyeonggi, denoted as "Current" in Table 8. The second and third baselines are the results of S-APPM introduced in Section 3, denoted as "Seoul Only S-APPM" and "Gyeonggi Only S-APPM." "Seoul Only S-APPM" refers to the results of S-APPM when only the intra-zonal passenger demand in Seoul is considered as in Section 4, and

Table 7
Model parameters used for the case study.

Variable		Units	Value
R	R_s	[km^2]	605.24
	R_g	[km^2]	2799.20
L	l_{ss}	[km]	14.76
	l_{sg}	[km]	25.48
	l_{gs}	[km]	25.48
	l_{gg}	[km]	31.74
V	$v_{ss,min}$, $v_{ss,max}$	[km/hr]	18.0, 40.0
	$v_{sg,min}$, $v_{sg,max}$	[km/hr]	25.0, 35.0
	$v_{gs,min}$, $v_{gs,max}$	[km/hr]	25.0, 35.0
	$v_{gg,min}$, $v_{gg,max}$	[km/hr]	20.0, 50.0
p		-	0.95
q		-	0.95
α		-	2
I		-	1
H		-	2
κ		-	0.5
T_0		[hr]	1/60
C	C_m	[\$/veh/day]	35.616
	C_x	[\$/stations/day]	1
	$C_{y,s}$	[\$/spaces/day]	4.73
	$C_{y,g}$	[\$/spaces/day]	0.24

"Gyeonggi Only S-APPM" refers to the results of S-APPM when only the intra-zonal passenger demand in Gyeonggi is considered.

In Table 8, it can be seen that x_s increased while x_g decreased in both demand scenarios. Since x is proportional to the squared reciprocal of $T^1_{A,t}$, this result implies that the average passenger waiting time in Seoul decreased and the average passenger waiting time in Gyeonggi increased when the two zones were considered together. The results of y are notable. In both demand scenarios, the density of parking spaces in Seoul (y_s) increased slightly, while the density of parking spaces in Gyeonggi (y_g) increased significantly. This shows that increasing the number of parking spaces in Gyeonggi is more cost-efficient than increasing the number of parking spaces in Seoul. These results show that T-APPM is capable of incorporating different cost variables across two regions so that the most cost-efficient solution can be derived. The densities of parking spaces in both Seoul and Gyeonggi are significantly less than the "Current" values of Seoul and Gyeonggi. This result implies that if the SAV system is introduced, the number of parking spaces will be significantly reduced. As a result of changes in x and y, the average number of parking spaces at each parking station in Seoul z_s changed slightly, while that of Gyeonggi z_g increased significantly. From this result, it can be concluded that, with the SAV system, it is more cost-efficient to have fewer parking stations with greater numbers of parking spaces, and especially to install more parking spaces in suburbs, which have lower land costs, reducing overall cost. Both m_s and m_g increase in T-APPM results because of increases in passenger demand. However, the results show that, compared to the "Current" situation, it is possible to significantly decrease the total number of vehicles by using the SAV system. Even when SAV replaces all passenger modes, including train, bus, and subway, and serves as a primary mode of passenger trips (i.e., the result of Passenger Demand by All-Mode, shown in Table 8), the total number of vehicles is still less than the "Current" value, which is currently only used for passenger demand by personal vehicles.

Table 8
Summary of results of Case Study for T-APPM

Demand Type	Variable		Current	Seoul Only S-APPM	Gyeonggi Only S-APPM	T-APPM
Passenger Demand by Personal Vehicle	x_s	[stations/km^2]	524.09	11.66	-	13.36
	x_g	[stations/km^2]	97.92	-	10.32	8.16
	y_s	[spaces/km^2]	7,150.72	718.22	-	820.12
	y_g	[spaces/km^2]	1740.12	-	175.66	366.54
	z_s	[spaces/station]	13.64	61.59	-	61.39
	z_g	[spaces/station]	17.77	-	17.01	44.90
	m_s	[veh]	2,703,429	477,944	-	605,699
	m_g	[veh]	4,394,130	-	536,827	1,327,406
	m	[veh]	7,097,559	-	-	1,933,105
Passenger Demand by All Mode	x_s	[stations/km^2]	524.09	27.512	-	28.54
	x_g	[stations/km^2]	97.92	-	17.68	13.12
	y_s	[spaces/km^2]	7,150.72	3728.66	-	3758.08
	y_g	[spaces/km^2]	1740.12	-	469.24	640.92
	z_s	[spaces/station]	13.64	135.52	-	131.68
	z_g	[spaces/station]	17.77	-	26.53	48.85
	m_s	[veh]	2,703,429	2,549,647	-	2,583,452
	m_g	[veh]	4,394,130	-	1,460,981	2,344,356
	m	[veh]	7,097,559	-	-	5,123,078

7. Conclusion

This study presents two analytical models to describe parking operations for SAVs in a given urban transportation system: the Single-zone Analytical Parking Planning Model (S-APPM) and the Two-zone Analytical Parking Planning Model (T-APPM). S-APPM assumes that the given traffic network is a single network with homogeneous network characteristics and passenger demand. On the other hand, T-APPM assumes that the given traffic network contains two separate zones, usually the city center and suburb. Both models are carefully derived based on the general model of demand-responsive transportation services (Daganzo and Ouyang, 2019a), introducing novel concepts such as parking and relocation. S-APPM offers a closed-form solution for parking operation scenarios with single-zone intra-zonal passenger trips. Consequently, computational complexity is significantly reduced compared to previously studied simulation-based methodologies. Extending S-APPM, T-APPM introduces inter-zonal passenger trips and the relocation of vehicles. The solution of the case study for T-APPM shows that this model can incorporate different macroscopic characteristics across two zones.

The contribution of this study is that two models allow policy-makers and decision-makers to plan parking operations under the dominance of Shared Autonomous Vehicles, yielding approximated numbers for both densities of parking stations and parking spaces. Using the proposed models to find optimal operational variables is much simpler than using previously studied simulation-based approaches. The simulation-based methods require much effort and time to set the simulation environment and run the simulation with different variables. However, the solutions from the proposed models can be derived in much less time and have much less complexity.

There are several assumptions made during the model derivations; these assumptions can be further studied so that the model can be made more realistic. As discussed in Section 3.2, it is possible to allocate a new passenger request to an SAV cruising back to the parking station (state C). The dotted line in Figure 2 indicates this state transition. Introducing this state transition would improve the efficiency of the whole system and, as a result, results will be better with a smaller SAV fleet and fewer parking spaces. Forcing SAVs to park between trips might add eVMT to the system and inflate congestion. This is particularly relevant in urban areas where traffic and parking are already pressing issues. One possible workaround to address this concern is to introduce state-specific cost variables into the model, which would allow for more targeted optimization of the system. These variables could account for the costs associated with eVMT and parking. By incorporating state-specific cost variables, we can fine-tune the model to optimize the allocation of SAVs and the distribution of parking stations and spaces. With a proper configuration, we expect that our model will increase the density of parking stations and parking spaces to ensure that the deadheading eVMT is not significant. This approach could lead to more efficient SAV operations that minimize congestion, better utilize parking resources, and provide a more realistic representation of SAV deployments in urban environments. Another way to reduce eVMT and potentially alleviate congestion is to incorporate the effect of Dynamic Ride Sharing (DRS) into the model. DRS enables multiple passengers with similar origins and destinations to share a single SAV, thus optimizing the allocation of SAVs and reducing the overall fleet size required. By integrating DRS into the model, it is possible to achieve a more efficient SAV operation that minimizes empty VMT, optimizes parking resources, and mitigates the impact on urban traffic. While the current model mainly focuses on systems without ridesharing, it can easily be integrated with the framework proposed by Daganzo and Ouyang (2019a) to incorporate the effect of DRS, making it a valuable foundation for future research. Figure 10 shows our suggestion for future researchers to incorporate DRS into our model. In this figure, the numbers within each node represent a vehicle's workload, characterized by a tuple of non-negative integers (i, j). The first index, i, denotes the number of passengers currently inside the vehicle, while the second index, j, indicates the number of passengers assigned to the vehicle for future pick-up. By incorporating these indices into the model, it is possible to track the allocation of SAVs more accurately and efficiently, taking into account the real-time status of each vehicle as it serves multiple passengers simultaneously through dynamic ride-sharing.

Also, it is assumed in T-APPM that SAVs are relocated to other zones only from state C. However, it is also realistic to assume that relocation of vehicles can happen from state P. This change can improve the model by dealing with cases in which extreme relocation of vehicles is required, and vehicles parked in one zone must be relocated to the other zone. Also, we used several approximations in both case studies in Section 4 and Section 6. The results of the case studies can be more realistic if we use field-observed values instead of approximated values. Using urban vehicle trajectory data is desirable to achieve adequate values for each parameters (Naveh and Kim, 2018; Choi et al., 2021; Jin et al., 2022). Additionally, while we assumed that SAVs would be equipped with advanced sensors and communication technologies, such as 5G networks, which are necessary for real-time data transmission and vehicle-to-vehicle communication, we did not explicitly consider the cost-benefit of data transfer for one vehicle in our study.

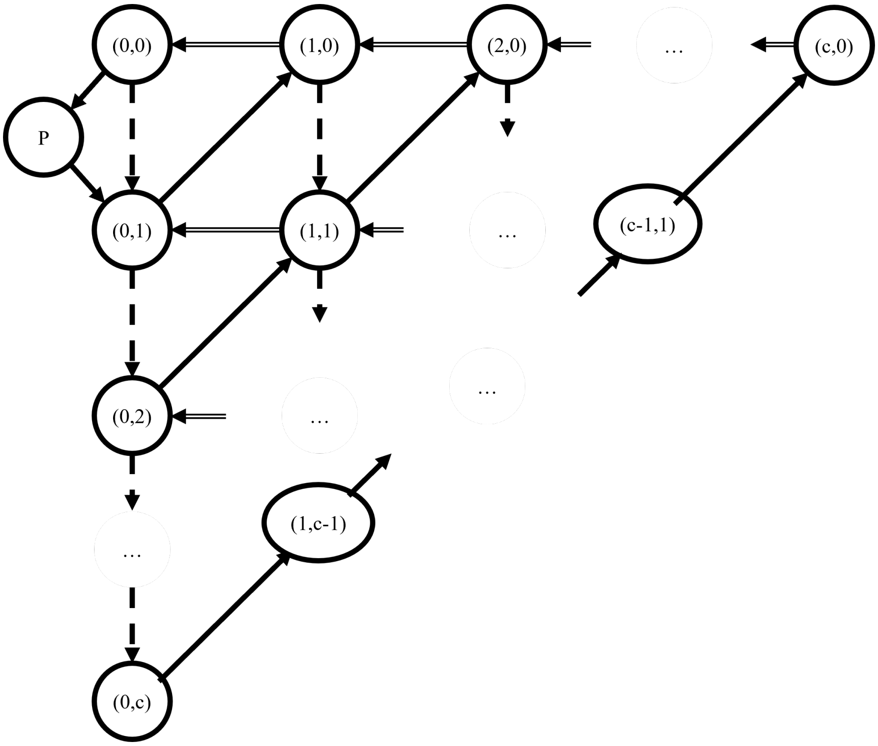

Figure 10: Modified workload transition network when incorporating the effect of Dynamic Ride Sharing into the model proposed in this study. Vehicle's workload is characterized by a tuple of non-negative integers (i, j). The first index, i, denotes the number of passengers currently inside the vehicle, while the second index, j, indicates the number of passengers assigned to the vehicle for future pick-up. By incorporating these indices into the model, it is possible to track the allocation of SAVs more accurately and efficiently, taking into account the real-time status of each vehicle as it serves multiple passengers simultaneously through dynamic ride-sharing.

Furthermore, while we acknowledge that the current energy crisis worldwide may affect the operating costs of SAVs, our study was intended to provide a general framework for parking planning with SAV fleets, rather than to conduct a comprehensive analysis of the impact of energy crises on SAVs. However, we recognize the importance of further research in this direction and will consider it in future work.

Future research can be conducted in various directions. In T-APPM, for simplicity of the model, we considered only inter-zonal passenger trips between two zones. However, T-APPM can be further investigated using a multi-zone approach. For example, we assumed in Sections 4 and 6 that the macroscopic characteristics of Seoul and Gyeonggi, such as passenger demand and costs, were homogeneous. However, Seoul and Gyeonggi can be split into multiple zones with different macroscopic characteristics. To create a "multi-zonal" analytical parking planning model, it is necessary to consider much more complex relocation between zone pairs. Developing a multi-zonal analytical parking planning model will contribute to addressing the inherent heterogeneity present in urban transportation systems. By incorporating spatial variations in demand, travel speeds, and infrastructure availability, a multi-zonal model can provide a more accurate representation of real-world dynamics and allow for more targeted optimization strategies. Such improvements will answer questions like 'Where exactly should parking stations be located?'

While the APPM may be particularly useful for new developments or greenfield sites, it can also be applied to existing cities with some modifications. In these cases, the model can be used to identify areas where parking demand is high or where there is a shortage of parking spaces, and to evaluate different planning scenarios and their impacts on parking supply and demand. In addition, since most SAVs are likely to be electric vehicles (EV), it is also necessary to consider battery and charging infrastructure (Lee et al., 2021) when planning the parking operation. In the incoming era of SAVs, parking stations will serve as storage places for unused vehicles and as depots that manage overall SAV operation, including charging. As a result, incorporating existing studies on the battery cycle of EVs and the charging infrastructure into parking operation is a good direction for future research.

CRediT authorship contribution statement

Seongjin Choi: Conceptualization, Methodology, Software, Formal analysis, Investigation, Resources, Data Curation, Writing - Original Draft, Visualization. **Jinwoo Lee:** Conceptualization, Methodology, Validation, Writing - Review & Editing, Funding acquisition.

References

Azevedo, C.L., Marczuk, K., Raveau, S., Soh, H., Adnan, M., Basak, K., Loganathan, H., Deshmunkh, N., Lee, D.H., Frazzoli, E., et al., 2016. Microsimulation of demand and supply of autonomous mobility on demand. Transportation Research Record 2564, 21–30.

Bahrami, S., Nourinejad, M., Nesheli, M.M., Yin, Y., 2022. Optimal composition of solo and pool services for on-demand ride-hailing. Transportation Research Part E: Logistics and Transportation Review 161, 102680.

Bates, J., Leibling, D., 2012. Spaced out. Perspectives on parking policy 9.

Choi, S., Kim, J., Yeo, H., 2021. Trajgail: Generating urban vehicle trajectories using generative adversarial imitation learning. Transportation Research Part C: Emerging Technologies 128, 103091.

Daganzo, C.F., Ouyang, Y., 2019a. A general model of demand-responsive transportation services: From taxi to ridesharing to dial-a-ride. Transportation Research Part B: Methodological 126, 213–224.

Daganzo, C.F., Ouyang, Y., 2019b. Public transportation systems: Principles of system design, operations planning and real-time control. World Scientific.

Daganzo, C.F., Ouyang, Y., Yang, H., 2020. Analysis of ride-sharing with service time and detour guarantees. Transportation Research Part B: Methodological 140, 130–150.

Estrada, M., Salanova, J.M., Medina-Tapia, M., Robusté, F., 2021. Operational cost and user performance analysis of on-demand bus and taxi systems. Transportation Letters 13, 229–242.

Fagnant, D.J., Kockelman, K.M., 2014. The travel and environmental implications of shared autonomous vehicles, using agent-based model scenarios. Transportation Research Part C: Emerging Technologies 40, 1–13.

Fakhrmoosavi, F., Gurumurthy, K., Kockelman, K., Hunter, C., Dean, M., 2022. On- and off-street parking strategies and outcomes for shared autonomous vehicle fleet operations, in: TRB 102nd Annual Meeting, The National Academies of Sciences.

Golbabaei, F., Yigitcanlar, T., Bunker, J., 2021. The role of shared autonomous vehicle systems in delivering smart urban mobility: A systematic review of the literature. International Journal of Sustainable Transportation 15, 731–748.

Jin, Z., Kim, J., Yeo, H., Choi, S., 2022. Transformer-based map-matching model with limited labeled data using transfer-learning approach. Transportation Research Part C: Emerging Technologies 140, 103668.

Jones, E.C., Leibowicz, B.D., 2019. Contributions of shared autonomous vehicles to climate change mitigation. Transportation Research Part D: Transport and Environment 72, 279–298.

Jorge, D., Correia, G., 2013. Carsharing systems demand estimation and defined operations: a literature review. European Journal of Transport and Infrastructure Research 13.

Kim, M., Roche, A., 2021. Optimal service zone and headways for flexible-route bus services for multiple periods. Transportation Planning and Technology 44, 194–207.

Kim, M.E., Levy, J., Schonfeld, P., 2019. Optimal zone sizes and headways for flexible-route bus services. Transportation Research Part B: Methodological 130, 67–81.

Ko, E., Kim, H., Lee, J., 2021. Survey data analysis on intention to use shared mobility services. Journal of Advanced Transportation 2021.

Kondor, D., Zhang, H., Tachet, R., Santi, P., Ratti, C., 2018. Estimating savings in parking demand using shared vehicles for home–work commuting. IEEE Transactions on Intelligent Transportation Systems 20, 2903–2912.

Kröger, L., Kickhöfer, B., 2017. Autonomous car-and ride-sharing systems: A simulation-based evaluation of various supply options for different regions .

Lam, W.H., Li, Z.C., Huang, H.J., Wong, S., 2006. Modeling time-dependent travel choice problems in road networks with multiple user classes and multiple parking facilities. Transportation Research Part B: Methodological 40, 368–395.

Lee, J., Shon, H., Papakonstantinou, I., Son, S., 2021. Optimal fleet, battery, and charging infrastructure planning for reliable electric bus operations. Transportation Research Part D: Transport and Environment 100, 103066.

Lees-Miller, J.D., 2016. Minimising average passenger waiting time in personal rapid transit systems. Annals of Operations Research 236, 405–424.

Lokhandwala, M., Cai, H., 2018. Dynamic ride sharing using traditional taxis and shared autonomous taxis: A case study of nyc. Transportation Research Part C: Emerging Technologies 97, 45–60.

Menon, N., Barbour, N., Zhang, Y., Pinjari, A.R., Mannering, F., 2019. Shared autonomous vehicles and their potential impacts on household vehicle ownership: An exploratory empirical assessment. International Journal of Sustainable Transportation 13, 111–122.

Narayanan, S., Chaniotakis, E., Antoniou, C., 2020a. Factors affecting traffic flow efficiency implications of connected and autonomous vehicles: A review and policy recommendations. Advances in Transport Policy and Planning 5, 1–50.

Narayanan, S., Chaniotakis, E., Antoniou, C., 2020b. Shared autonomous vehicle services: A comprehensive review. Transportation Research Part C: Emerging Technologies 111, 255–293.

Naveh, K.S., Kim, J., 2018. Urban trajectory analytics: day-of-week movement pattern mining using tensor factorization. IEEE Transactions on Intelligent Transportation Systems 20, 2540–2549.

Nourinejad, M., Bahrami, S., Roorda, M.J., 2018. Designing parking facilities for autonomous vehicles. Transportation Research Part B: Methodological 109, 110–127.

Oh, S., Seshadri, R., Azevedo, C.L., Kumar, N., Basak, K., Ben-Akiva, M., 2020. Assessing the impacts of automated mobility-on-demand through agent-based simulation: A study of singapore. Transportation Research Part A: Policy and Practice 138, 367–388.

Okeke, O.B., 2020. The impacts of shared autonomous vehicles on car parking space. Case Studies on Transport Policy 8, 1307–1318.

Pakusch, C., Meurer, J., Tolmie, P., Stevens, G., 2020. Traditional taxis vs automated taxis–does the driver matter for millennials? Travel Behaviour and Society 21, 214–225.

Papanikolaou, A., Basbas, S., 2021. Analytical models for comparing demand responsive transport with bus services in low demand interurban areas. Transportation Letters 13, 255–262.

Rodriguez-Bachiller, A., 1983. Errors in the measurement of spatial distances between discrete regions. Environment and Planning A 15, 781–799.

Shaheen, S., Chan, N., 2016. Mobility and the sharing economy: Potential to facilitate the first-and last-mile public transit connections. Built Environment 42, 573–588.

Wang, K., Zhang, W., 2021. The role of urban form in the performance of shared automated vehicles. Transportation Research Part D: Transport and Environment 93, 102744.

Wang, S., Correia, G.H.d.A., Lin, H.X., 2022. Assessing the potential of the strategic formation of urban platoons for shared automated vehicle fleets. Journal of Advanced Transportation .

Wilson, R.M., 1990. The average distance between two zones. Geographical Analysis 22, 348–360.

Yan, H., Kockelman, K.M., Gurumurthy, K.M., 2020. Shared autonomous vehicle fleet performance: Impacts of trip densities and parking limitations. Transportation Research Part D: Transport and Environment 89, 102577.

Zhang, W., 2017. The interaction between land use and transportation in the era of shared autonomous vehicles: A simulation model. Ph.D. thesis. Georgia Institute of Technology.

Zhang, W., Guhathakurta, S., 2017. Parking spaces in the age of shared autonomous vehicles: How much parking will we need and where? Transportation Research Record 2651, 80–91.

Zhang, W., Guhathakurta, S., Fang, J., Zhang, G., 2015. Exploring the impact of shared autonomous vehicles on urban parking demand: An agent-based simulation approach. Sustainable Cities and Society 19, 34–45.

Zhang, W., Wang, K., 2020. Parking futures: Shared automated vehicles and parking demand reduction trajectories in atlanta. Land Use Policy 91, 103963.

A. Glossary of Notations

Notation	Unit	Meaning
x	[stations/km^2]	density of parking stations
y	[spaces/km^2]	density of parking spaces
m	[veh]	number of SAV fleets
z	[spaces/stations]	the average number of parking spaces in a parking station
R	[km^2]	area of target area
$Cost$	[$/day]	overall daily average operation cost
$T_{A,t}$	[hr]	average passenger waiting time
$T^i_{A,t}$	[hr]	average travel time from the i-th nearest parking station to the origin of the passenger
T_0	[hr]	maximum allowed average passenger waiting time
C_x	[$/stations/day]	daily operation cost of a parking station
C_y	[$/spaces/day]	daily operation cost of a parking space
C_m	[$/vehicles/day]	daily operation cost of an SAV fleet
n_A	[veh]	the number of SAV fleets in state A
n_S	[veh]	the number of SAV fleets in state S
n_C	[veh]	the number of SAV fleets in state C
n_P	[veh]	the number of SAV fleets in state P
n^{req}_A	[veh]	the required number of SAV fleets in state A
n^{req}_S	[veh]	the required number of SAV fleets in state S
n^{req}_C	[veh]	the required number of SAV fleets in state C
n^{req}_P	[veh]	the required number of SAV fleets in state P
v_{min}	[veh]	the minimum average ground speed throughout the day
v_{max}	[veh]	the maximum average ground speed throughout the day
λ_t	[veh/hr/km^2]	average passenger demand in time window t
l_t	[km]	average trip length
v_t	[km/hr]	average ground speed in time window t
$T_{S,t}$	[veh]	average travel time for passenger trip
$T_{C,t}$	[veh]	average travel time from the destination of the passenger to the nearest parking station
$T^i_{C,t}$	[veh]	average travel time from the destination of the passenger to the i-th nearest parking station
p	-	confidence level to guarantee that the passengers are assigned to the nearest parking station at a certain confidence level.
q	-	confidence level guarantee that the nearest parking station is not full.
α	-	the incremental ratio of the travel time to the next nearest parking station
H	[hr]	length of a time window
I	-	the mean-to-variance ratio of the number of fleets parked at each parking station

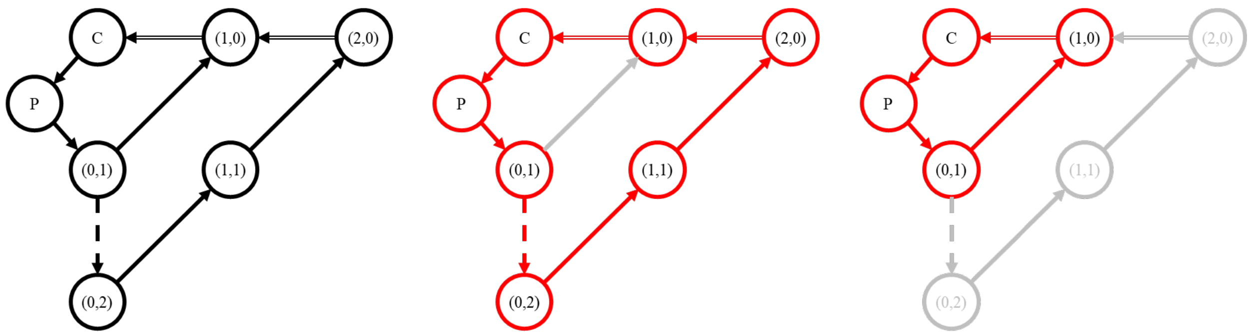

(a) Workload transition network (b) At $t_{\lambda_{max}}$ (c) At $t_{\lambda_{min}}$

Figure 11: Modified workload transition network when incorporating the effect of Dynamic Ride Sharing into the model proposed in this study. The vehicle's workload is characterized by a tuple of non-negative integers (i, j). The first index, i, denotes the number of passengers currently inside the vehicle, while the second index, j, indicates the number of passengers assigned to the vehicle for future pick-up. (a) Overall workload transition network, (b) Workload transition network at $t = t_{\lambda_{max}}$ (only red lines are considered), and (c) Workload transition network at $t = t_{\lambda_{min}}$ (only red lines are considered).

B. Integration of Dynamic Ride-Sharing in S-APPM

We consider a case where the maximum number of occupants in a vehicle is two people, following Daganzo and Ouyang (2019a). Figure 11 (a) shows the overall modified workload transition network. The vehicle's workload is characterized by a tuple of non-negative integers (i, j). The first index, i, denotes the number of passengers currently inside the vehicle, while the second index, j, indicates the number of passengers assigned to the vehicle for future pick-up.

In S-APPM in Section 3, we considered two distinct time windows: one during which the demand is at its peak ($t_{\lambda_{max}}$) and another during which the demand is at its lowest ($t_{\lambda_{min}}$). We analytically derived solutions by comparing the operational variables within these two time windows. Following a similar approach, we can make certain simplifications for the integration of pooling. Given that high demand at $t_{\lambda_{max}}$ implies a large number of individuals seeking to use SAVs, we can simplify the integration of pooling by assuming that during this time window, each SAV is consistently occupied by two passengers. This assumption aligns with the concept that when demand is high, the probability of finding passengers with similar routes increases, making pooling more efficient. Conversely, during the time window when the demand is at its minimum ($t_{\lambda_{min}}$), we can assume that SAVs are occupied by only one passenger. This assumption stems from the understanding that during periods of low demand, the likelihood of matching passengers with similar routes decreases. These assumptions enable us to form a basic analytical framework to understand the interaction between parking planning and pooling by focusing on how vehicle occupancy changes in response to fluctuations in demand. However, it is important to acknowledge that these assumptions are simplifications and that in real-world scenarios, demand and occupancy can vary in more complex patterns.

As a consequence of the assumptions regarding passenger occupancy during different demand periods, we can conceptualize the workload transition network for the SAVs. Specifically, at the time window $t_{\lambda_{max}}$, when demand is at its peak and each SAV is assumed to be occupied by two passengers, the workload transition network is assumed to take on the form depicted in Figure 11 (b) and only the red lines are considered as active state transitions. On the other hand, at the time window $t_{\lambda_{min}}$, when demand is at its lowest and each SAV is assumed to be occupied by a single passenger, the workload transition network is assumed to take on the form depicted in Figure 11 (c), which is identical to S-APPM.

The minimum required fleet size, or the maximum required number of SAVs, m^*, can be computed by summing the required number of vehicles at each state at $t_{\lambda_{max}}$ as follows:

$$
\begin{aligned}
& m^* = \max_t (m^{req}(t)) = m^{req}(t_{\lambda_{max}}) \\
& m^{req}(t_{\lambda_{max}}) = n_{01}^{req}(t_{\lambda_{max}}) + n_{02}^{req}(t_{\lambda_{max}}) + n_{11}^{req}(t_{\lambda_{max}}) + n_{20}^{req}(t_{\lambda_{max}}) + n_{10}^{req}(t_{\lambda_{max}}) + n_{C}^{req}(t_{\lambda_{max}}) + n_{P}^{req}(t_{\lambda_{max}})
\end{aligned}
. \quad \text{(B.1)}
$$

The summation of $n_{01}^{req}(t_{\lambda_{max}})$ and $n_{02}^{req}(t_{\lambda_{max}})$ is equivalent to the number of SAV fleets in state A, denoted by $n_{A}^{req}(t_{\lambda_{max}})$, as presented in Section 3. This equivalence arises because the transition from states $(0,1)$ and $(0,2)$ to state $(1,1)$ involves the time it takes for the SAV at a parking station to be assigned to two passengers and then proceed to pick up one of them. As a result, the time spent in state $(0,1)$ and $(0,2)$ is essentially the travel time from the parking station to the origin location of the first passenger. While the unit passenger demand is represented by λ_{max}, the vehicle demand is effectively halved to $\frac{\lambda_{max}}{2}$. This is due to the assumption that there are two passengers in each vehicle as a result of pooling. Then, the summation of $n_{01}^{req}(t_{\lambda_{max}})$ and $n_{02}^{req}(t_{\lambda_{max}})$ can be calculated as follows:

$$n_{01}^{req}(t_{\lambda_{max}}) + n_{02}^{req}(t_{\lambda_{max}}) = \frac{\lambda_{max}R}{2} \cdot T_{A,t_{\lambda_{max}}}^{1}(p + \alpha p - \alpha p^2). \tag{B.2}$$

The time spent in state $(1,1)$ represents the travel time from the origin location of the first passenger to the origin location of the second passenger. This travel time can be calculated analytically using the expression for the expected distance to the closest of n random points, as presented in Section 7.A of Daganzo and Ouyang (2019b). As a result, the number of SAV fleets in the state (1,1) can be calculated as follows:

$$\begin{aligned} n_{11}^{req}(t_{\lambda_{max}}) &= \frac{\lambda_{max}R}{2} \cdot \sqrt{\frac{R}{n_{01}^{req}(t_{\lambda_{max}}) + n_{02}^{req}(t_{\lambda_{max}})}} \cdot \frac{\kappa}{v_{min}} \\ &= \frac{\lambda_{max}R}{2} \cdot \sqrt{\frac{2}{\lambda_{max} \cdot (p + \alpha p - \alpha p^2)}} \cdot \frac{\kappa}{v_{min}} \cdot \sqrt{\frac{1}{T_{A,t_{\lambda_{max}}}^{1}}}. \end{aligned} \tag{B.3}$$

Once the second passenger boards, the vehicle moves to the closer destination and drops off one, during state $(2,0)$. It then continues to the destination of the remaining passenger, during state $(1,0)$. The average travel time between the second pick-up and the last drop-off is higer than a single passenger trip without ridesharing, $l_{t_{\lambda_{max}}}/v_{min}$. The ratio between these two average in-service travel times is denoted by $\gamma_{t_{\lambda_{max}}} > 1$. Note that in the setting of Daganzo and Ouyang (2019a), it is $1 + \frac{1}{\sqrt{2}}$. The in-service SAV fleet size is:

$$n_{10}^{req}(t_{\lambda_{max}}) + n_{20}^{req}(t_{\lambda_{max}}) = \gamma_{t_{\lambda_{max}}} \cdot \frac{\lambda_{max}R}{2} \cdot \frac{l_{t_{\lambda_{max}}}}{v_{min}}. \tag{B.4}$$

The number of SAV fleets in state C and P should be equivalent to the derivation from Section 3 as follows:

$$\begin{aligned} n_{C}^{req}(t_{\lambda_{max}}) &= \frac{\lambda_{max}R}{2} \cdot T_{A,t_{\lambda_{max}}}^{1} \\ n_{P}^{req}(t_{\lambda_{max}}) &= \kappa\Phi^{-1}(p)\sqrt{\lambda_{max}RHI}\frac{1}{v_{min}T_{A,t_{\lambda_{max}}}^{1}}. \end{aligned} \tag{B.5}$$

As a result,

$$\begin{aligned} m^* =& \frac{\lambda_{max}R}{2}(1 + p + \alpha p - \alpha p^2) \cdot T_{A,t_{\lambda_{max}}}^{1} + \frac{\lambda_{max}R}{2} \cdot \sqrt{\frac{2}{\lambda_{max} \cdot (p + \alpha p - \alpha p^2)}} \cdot \frac{\kappa}{v_{min}} \cdot \sqrt{\frac{1}{T_{A,t_{\lambda_{max}}}^{1}}} \\ &+ \gamma_{t_{\lambda_{max}}} \cdot \frac{\lambda_{max}R}{2} \cdot \frac{l_{t_{\lambda_{max}}}}{v_{min}} + \kappa\Phi^{-1}(p)\sqrt{\lambda_{max}RHI}\frac{1}{v_{min}T_{A,t_{\lambda_{max}}}^{1}} \end{aligned}. \tag{B.6}$$

For the case where the demand is at its minimum, the derivation can proceed in the same manner as in the original Single-Zone Analytical Parking Planning Model (S-APPM). As a result, we can derive the optimal density of parking spaces following Equation 3.19 and Equation 3.20.

Since m^* has $\sqrt{\frac{1}{T^1_{A,t_{\lambda_{max}}}}}$ term inside, Equation 3.22 would be updated with an additional term, which is $P'_{-\frac{1}{2}}\left(T^1_{A,t_{\lambda_{max}}}\right)^{-\frac{1}{2}}$ as follows:

$$\min_{T^1_{A,t_{\lambda_{max}}}} Cost\left(T^1_{A,t_{\lambda_{max}}}\right) = \min_{T^1_{A,t_{\lambda_{max}}}} \left(P'_0 + P'_{-2}\left((T^1_{A,t_{\lambda_{max}}})\right)^{-2} + P'_{-1}\left(T^1_{A,t_{\lambda_{max}}}\right)^{-1} + P'_1 T^1_{A,t_{\lambda_{max}}} + P'_{-\frac{1}{2}}\left(T^1_{A,t_{\lambda_{max}}}\right)^{-\frac{1}{2}}\right). \tag{B.7}$$

The inclusion of the term $\left(T^1_{A,t_{\lambda_{max}}}\right)^{-\frac{1}{2}}$ introduces additional complexity to Equation B.7. As a consequence, finding an analytical closed-form solution for this equation becomes increasingly challenging. However, this equation can still be numerically solved.